THE JOURNAL OF BIOLOGICAL CHEMISTRY VOL. 287, NO. 38, pp. 31725–31738, September 14, 2012

Redox Modulation of Flavin and Tyrosine Determines Photoinduced Proton-coupled Electron Transfer and Photoactivation of BLUF Photoreceptors[S]

Received for publication, June 14, 2012, and in revised form, July 24, 2012 Published, JBC Papers in Press, July 25, 2012, DOI 10.1074/jbc.M112.391896

Tilo Mathes[‡1,2], **Ivo H. M. van Stokkum**[‡], **Manuela Stierl**[§], **and John T. M. Kennis**[‡3]

From the [‡]*Biophysics Group, Department of Physics and Astronomy, Faculty of Sciences, Vrije Universiteit, De Boelelaan 1081A, 1081 HV, Amsterdam, The Netherlands and the* [§]*Institut für Biologie, Experimentelle Biophysik, Humboldt Universität zu Berlin, Invalidenstrasse 42, D-10115 Berlin, Germany*

Background: Proton-coupled electron transfer is the key step in BLUF photoactivation.
Results: Redox modulation of flavin and tyrosine determines electron transfer rates and signaling efficiency and reveals a new photocycle intermediate.
Conclusion: Partial charge transfer from tyrosine to flavin takes place prior to full electron transfer.
Significance: Mechanistic details of protein-modulated electron transfer processes are crucial to understand biological proton-coupled electron transfer reactions.

Photoinduced electron transfer in biological systems, especially in proteins, is a highly intriguing matter. Its mechanistic details cannot be addressed by structural data obtained by crystallography alone because this provides only static information on a given redox system. In combination with transient spectroscopy and site-directed manipulation of the protein, however, a dynamic molecular picture of the ET process may be obtained. In BLUF (blue light sensors using FAD) photoreceptors, proton-coupled electron transfer between a tyrosine and the flavin cofactor is the key reaction to switch from a dark-adapted to a light-adapted state, which corresponds to the biological signaling state. Particularly puzzling is the fact that, although the various naturally occurring BLUF domains show little difference in the amino acid composition of the flavin binding pocket, the reaction rates of the forward reaction differ quite largely from a few ps up to several hundred ps. In this study, we modified the redox potential of the flavin/tyrosine redox pair by site-directed mutagenesis close to the flavin C2 carbonyl and fluorination of the tyrosine, respectively. We provide information on how changes in the redox potential of either reaction partner significantly influence photoinduced proton-coupled electron transfer. The altered redox potentials allowed us furthermore to experimentally describe an excited state charge transfer intermediately prior to electron transfer in the BLUF photocycle. Additionally, we show that the electron transfer rate directly correlates with the quantum yield of signaling state formation.

BLUF (blue light receptors using FAD) proteins are responsible for photoadaptive responses of many prokaryotes and a few eukaryotes (1, 2). These blue light induced reactions vary from phototaxis (3, 4) and photosynthetic gene regulation (5, 6) in phototrophic organisms to biofilm formation (7) and even virulence (8) in pathogenic bacteria. These receptor proteins are modularly designed and contain the ~150-amino acid large flavin-binding BLUF domain to modulate the activity of their corresponding effector domain. In many cases, the effector domain is directly fused to the receptor. Lately, these BLUF-coupled effectors, predominantly BLUF domain-regulated enzymes, have been successfully used as so-called optogenetic tools to manipulate, for example, the second messenger level in a given cell (type) by application of light (9–12). Still, the photoactivation mechanism and communication between receptor and effector are not well understood. After excitation with blue light, proton-coupled electron transfer (PCET)[4] from a nearby, conserved tyrosine side chain (Tyr-8 (*Y8*) in Fig. 1*B*) to the flavin takes place (13). In the dark-adapted state, this reaction occurs in a strictly sequential order of electron transfer followed by proton transfer, whereas in the light-adapted state, a highly concerted electron and proton transfer reaction leads to the formation of the same neutral flavin/tyrosine radical pair (13–16). The neutral radical pair recombines to the oxidized state, which results in a rearrangement of the hydrogen bond network mainly between flavin, tyrosine, and a conserved glutamine residue. The rearranged hydrogen bond network is characterized by a downshift of carbonyl vibrations of the flavin, thus indicating a stronger hydrogen bond coordination at this functional group (17, 18). This is most likely predominantly facilitated by the rotation of the glutamine amide side chain (19, 20) and leads to the red-shifted absorbance spectrum of the light-adapted state (5). Additionally, an unusually strong

[S] This article contains supplemental Figs. S1–S4.

[1] Supported by the Chemical Sciences Council of the Netherlands Organization for Scientific Research through an ECHO grant (to J. T. M. K.), the LaserLab Europe access program (LCVU-1618), and the Deutsche Forschungsgemeinschaft.

[2] To whom correspondence should be addressed. Tel.: 31-20-59-87935; E-mail: t.mathes@vu.nl.

[3] Supported by the Chemical Sciences Council of the Netherlands Foundation for Scientific Research through a Vici grant.

[4] The abbreviations used are: PCET, proton-coupled electron transfer; EADS, evolution-associated difference spectra; GSB, ground state bleach; ESA, excited state absorption; SE, stimulated emission; SADS, species-associated difference spectra; CT, charge transfer; ET, electron transfer.

hydrogen bond is formed from the conserved tyrosine to the glutamine side chain (19, 21). The molecular details of both dark- and light-adapted states as well as the implications for signal transduction are still under heavy debate because the available crystal structures of BLUF domains gave contradicting results, especially on the orientation of the glutamine side chain (22–27). Additionally, theoretical calculations indicate that a tautomerization of the glutamine side chain is another possible hydrogen bond switch mechanism, which is, however, still lacking hard experimental proof (28–31). The hydrogen bond switched stated is also considered to be representative for the biologically active state. Still, the structural changes (most likely induced by the hydrogen bond switch) that facilitate biological signaling by changes in the interaction of the BLUF domain with other proteins or directly fused effector domains are very small and poorly understood. So far only one structure of a BLUF-effector complex has been solved and a model for signal transduction has been established (22). It is very likely, however, that there are various molecular ways of signaling in BLUF photoreceptors similar to what is known about Light-Oxygen-Voltage (LOV) domain signaling (32).

In this article, we address the very first reaction after blue light excitation in the BLUF domain: photoinduced electron transfer. In addition to their very intriguing signal transduction aspect, BLUF domains are also very powerful model systems to study PCET. PCET involving a tyrosine side chain is a key reaction in the oxygen-evolving photosystem II complex and up to now is not fully understood (33–35). Most model studies in this field are carried out using small heavy metal complexes or modified cytochrome *c* or azurin proteins. In contrast to these artificial model systems, BLUF domains present the smallest so far investigated evolutionarily optimized model system to study PCET. In a previous publication (15), we addressed the effects of hydrogen bonding in dark- and light-adapted states on the sequence of electron and proton transfer. In the light-adapted state, we observed a highly efficient proton transfer reaction concerted with electron transfer within 1 ps. In the dark-adapted state, proton transfer lags electron transfer by (tens of) picoseconds. Thus, the light-adapted state is preconfigured for proton transfer. Here we address the differences in photoinduced electron transfer between various BLUF domains. Although all BLUF domains are very similar in structure and sequence of the flavin binding pocket, the ultrafast electron transfer varies from a few ps to hundreds of ps within the BLUF family (13, 14, 36–44). A major factor that determines electron transfer in chemistry and biology is the relative redox potentials of the reaction partners. Previously, Ishikita (45) reported a theoretical study on the redox potential of the one-electron reduction of FMN in flavodoxin and its susceptibility to the protein environment. In a later study, he addressed the effects of the hydrogen bond network in AppA on the redox potential of the reactive tyrosine (46). Accordingly, we observe here that modulation of the redox potential of both flavin and tyrosine significantly influences the rate of electron transfer. Due to these altered kinetic properties, the observation of a previously occluded excited state charge transfer intermediate is facilitated. Selected mutations and modifications were introduced into Slr1694 (also referred to as SyPixD) from *Synechocystis* sp. PCC 6803 and studied by ultrafast spectroscopy.

TABLE 1
Oligonucleotides used for *in frame* deletion of *tyrA*
Regions homologous to *tyrA* are shown in boldface type.

Primer	Sequence (5′ → 3′)
DtyrA-5′	**GGATCTGAACGGGCAGCTGACGGCTCGCGTGGCTTAAGAGGTTTA TTATG**GTGTAGGCTGGAGCTGCTTC
DtyrA-3′	**GATGATGTGAATCATCCGGCACTGGATTATTACTGGCGATTGTCA TTCGC**CGGCTGACATGGGAATTAGC

EXPERIMENTAL PROCEDURES

Expression Strain Generation and Characterization—CmpX13 (47) was rendered tyrosine-auxotrophic by in-frame deletion of *tyrA* according to established homologous recombination protocols (48). A linear double-stranded DNA fragment containing a kanamycin resistance conferring cassette flanked by FLP recombinase recognition target sites was amplified by PCR from pKD4 (49), including a 50-bp homology region flanking the *tyrA* gene at the 5′- and 3′-end using the primers DtyrA-5′ and DtyrA-3′ (Table 1). After transformation of the recipient strain, clones were selected on kanamycin containing LB-agar and colony-purified. Successful disruption of the *tyrA* gene was confirmed by growth tests in minimal media with and without the addition of L-tyrosine. The genomically integrated kanamycin resistance-conferring cassette of a single correctly identified clone was removed by expression of FLP recombinase according to protocols described previously (47, 49). The resulting clones were colony-purified and selected for kanamycin sensitivity and tyrosine auxotrophy. A single clone, henceforth named CpXΔY, was verified by DNA sequence analysis and used for protein production as indicated below.

The tyrosine requirement of CpXΔY was determined relative to the glucose consumption. Cells were grown in M9 minimal medium under glucose-limiting conditions (0.1% (w/v)) with varying concentrations of L-tyrosine. The cell density was estimated by absorbance measurements at 600 nm every 20 min during growth in a 96-well plate shaking incubator at 37 °C. After reaching the stationary phase, the L-tyrosine minimal requirement was extracted at concentrations slightly below the maximum growth level in apparent L-tyrosine non-limiting conditions (not shown).

Mutants and Protein Production—Slr1694 mutants were produced from pET28(+)-*slr1694*, as described previously (44). Site-directed mutations were introduced according to the QuikChange™ (Stratagene) protocol using the primer pairs N31R/N31R_r and N31H/N31H_r as indicated (Table 2). Mutations were confirmed by restriction digestion and DNA sequence analysis. The flavin composition of the purified, mutated proteins was determined by HPLC, as described previously (47, 50).

Homology Modeling—Homology models of the two Asn-31 mutants were created using the Swiss-Model server (51) on the basis of the Slr1694 crystal structure (23).

Fluorotyrosine Labeling—For incorporation of 3-fluorotyrosine (AstaTech, Inc.) and 2-fluorotyrosine (Matrix Scientific), a fed-batch fermentation protocol was established. CpXΔY cells transformed with pET28a(+)-*slr1694* were grown

TABLE 2
Oligonucleotides used for site-directed mutagenesis on Slr1694
Mismatched base pairs corresponding to the changed amino acid codons are shown in boldface type.

Primer	Sequence (5′ → 3′)
N31R	CTTAGAATCTTCCCAAAGA**CG**TAATCCGGCCAATGGC
N31R_r	GCCATTGGCCGGATTA**CG**TCTTTGGGAAGATTCTAAG
N31H	CTTAGAATCTTCCCAAAGA**C**ATAATCCGGCCAATGGC
N31H_r	GCCATTGGCCGGATTAT**G**TCTTTGGGAAGATTCTAAG

in M9 minimal medium supplemented with 50 μM riboflavin and unfluorinated L-tyrosine in a 500-ml fermentation vessel (Multifors reactor, Infors HT AG, Basel) at 37 °C with percolation of pressurized air and gentle agitation. By monitoring the pO_2 level of the medium via an oxygen electrode, the metabolic activity of the cells was observed indirectly. Upon consumption of essential nutrients (glucose, ammonia, tyrosine) the pO_2 level rises abruptly because oxidative phosphorylation comes to a halt, and the cells start to enter a stationary phase. This event was used to lower the temperature to 26 °C and to start feeding new carbon and nitrogen sources as well as the fluorotyrosine analogs (160 mg/liter). The protein production was induced by the addition of 1 mM isopropyl 1-thio-β-D-galactopyranoside shortly after. The cells were further cultivated for about 13 h under these conditions and harvested subsequently. Protein preparation from these cells was carried out as described previously.

Spectroscopy—Steady state spectra were recorded on a two-beam scanning UV-visible photometer (Cary300bio, Varian). Dark state recovery was measured at 493 nm after blue light illumination using an LED (Luxeon Lumiled, 450 nm, 1 watt).

Ultrafast Transient Absorption Spectroscopy and Data Analysis—Visible absorption spectroscopy was carried out using pump-probe setups as described previously (44, 52). The reaction was induced at 400 nm with an energy of ~800 nJ/pulse. In order to prevent multiple excitations of the same molecule, the sample was put between two windows separated by a 200-μm spacer and moved perpendicularly to the probe beam in a Lissajous motion as described previously (14). Before analysis, a preprocessing method was applied to data sets to correct for the pre-time 0 signal by subtraction of the average pre-time 0 signal at each wavelength. The time-resolved data can be described in terms of a parametric model in which some parameters, such as those descriptive of the instrument response function, are wavelength-dependent, whereas others, such as the lifetime of a certain spectrally distinct component, underlie the data at all wavelengths. The presence of parameters that underlie the data at all wavelengths allow the application of global analysis techniques (53), which model wavelength-invariant parameters as a function of all available data. The partitioned variable projection algorithm is well suited to the optimization of model parameters for global analysis models (54). The algorithm has the further advantage of estimating the S.E. of parameter estimates, an advantage that is useful in model selection and validation. A compartmental model was used to describe the evolution of the spectrally distinct components in time. Global analysis was then applied to estimate the lifetime and relative concentration of each component at each wavelength in the data. All data analyses were carried out using TIMP (54) and the Glotaran software package (55).

RESULTS

Positively Charged Amino Acids Close to C2=O Increase Cofactor Selectivity in Slr1694—Mutations N31H and N31R close to the C2=O carbonyl group of the isoalloxazine ring of the flavin were successfully introduced into the BLUF domain of Slr1694. Both mutated proteins show wild type-like ground state absorption in the dark-adapted state, slightly shifted by 3 (N31R) and 4 nm (N31H) (50). The dark recovery is slowed down by a factor of about 4 in both mutants to about 28 s (N31H) and 29 s (N31R). Despite their similarity to AppA (N31H) and BlrB (N31R), the dark recovery seems not to be influenced strongly by these mutations alone. In the AppA-like N31H mutant, a drastic slowing down of the dark recovery was expected, whereas in the BlrB-like N31R mutant, a behavior similar to that of Slr1694 WT was expected. Interestingly, the introduction of a positive charge at this position led to a preferential binding of FMN and FAD in the BLUF domain of both Asn-31 mutants (50); BLUF domains heterologously expressed in *Escherichia coli* usually show a quite heterogenous flavin composition with similar amounts of riboflavin, FMN, and FAD bound to the photoreceptor domain (47, 56). In the N31R and N31H mutants, the amount of riboflavin was below the detection level. From the homology models of the two mutant proteins, the changed residues are within hydrogen bonding distance of the C2=O carbonyl of the flavin (Fig. 1*C*). Additionally, the groups are close to the negatively charged phosphate group of the flavin, thus supporting its coordination by Arg-30, a semiconserved residue in the BLUF family, which is present in neither BlrB nor AppA.

Fluorotyrosine Labeling of Slr1694—2- or 3-fluoro-L-tyrosine was exclusively incorporated into the BLUF domain using a custom-made tyrosine auxotrophic strain to prevent biosynthesis of unfluorinated tyrosine, which would compete most likely successfully with the tyrosine analog. In combination with a fed-batch procedure, high cell density was achieved along with complete consumption of the supplemented L-tyrosine before fluorinated tyrosine was added and the protein production was induced. After induction with isopropyl 1-thio-β-D-galactopyranoside, the cells, if supplemented with natural tyrosine, usually double about once during the following protein production phase (not shown). However, after supplementation with fluorotyrosine, the cell density increased only by about 50%, indicating some interference with cell metabolism. The purified 2- and 3-fluorotyrosine-labeled BLUF domains showed WT-like dark state absorbance spectra (Fig. 2*A*). The dark recovery after blue light excitation was slowed down by a factor of about 4 in 2-fluorotyrosine-labeled Slr1694 (SlrY2F) to about 40 s, whereas 3-fluorotyrosine-labeled Slr1694 (SlrY3F) was only slightly affected (Fig. 2*B*).

Ultrafast Dynamics of Mutant and Modified Slr1694 BLUF Domains—The N31R, N31H, SlrY2F, and SlrY3F proteins were investigated in H_2O buffer by transient absorption spectroscopy using 400-nm excitation and white light probe beams. Because the dark recovery reaction is also hydrogen/deuterium isotope-dependent and slowed down in D_2O, we were only able

A

	1								10								20								30				
Slr1694			M	S	L	Y	R	L	I	**Y**	S	S	Q	G	I	P	N	L	Q	P	Q	D	L	K	D	I	L	E	S	S	Q	R	**N**	N	P	A	N
AppA	12	G	S	D	L	V	S	C	C	**Y**	R	S	L	A	A	P	D	L	T	L	R	D	L	L	D	I	V	E	T	S	Q	A	**H**	N	A	R	A
BlrB		M	D	E	L	V	S	L	T	**Y**	R	S	R	V	R	L	A	D	P	V	A	D	I	V	Q	I	M	R	A	S	R	V	**R**	N	L	R	L
Tll0078			M	G	L	H	R	L	I	**Y**	L	S	C	A	T	D	G	L	S	Y	P	D	L	R	D	I	M	A	K	S	E	V	**N**	N	L	R	D
YcgF				M	L	T	T	L	I	**Y**	R	S	H	I	R	G	D	E	P	V	K	K	I	E	E	M	V	S	I	A	N	R	**R**	N	M	R	S

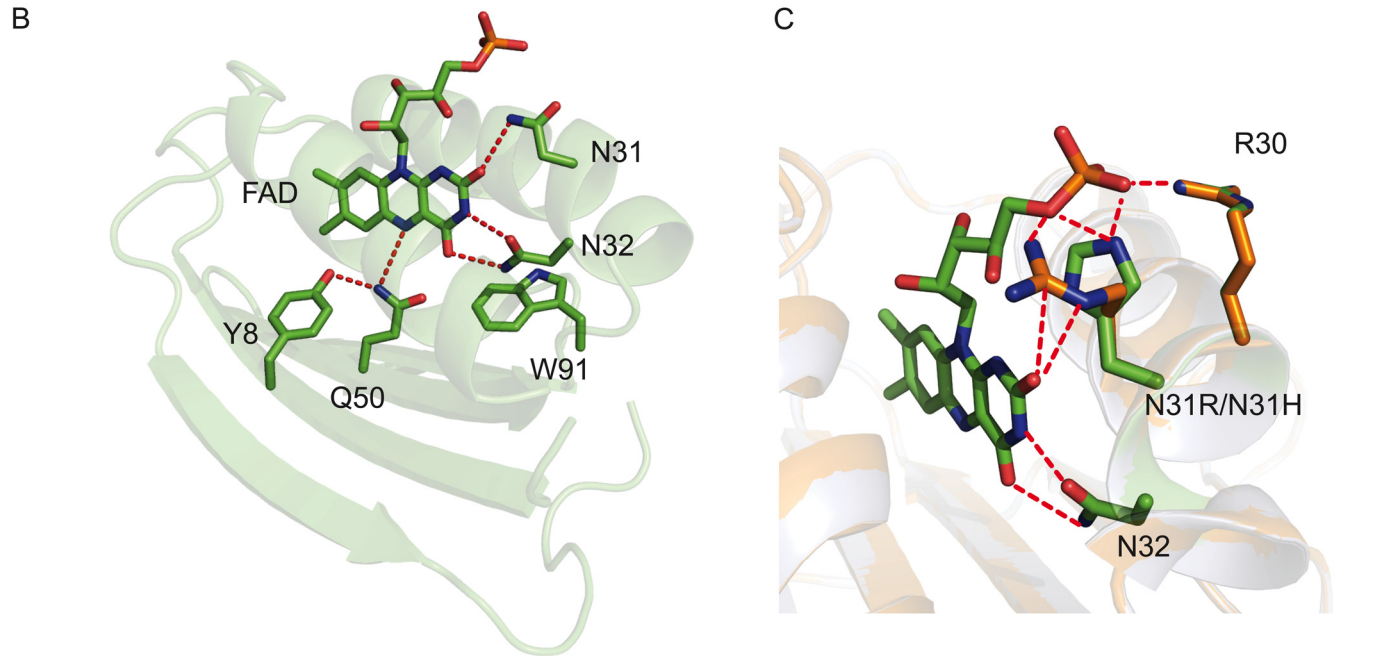

FIGURE 1. **Amino acid composition in selected BLUF domains.** *A*, sequence alignment of the first 35 amino acids in the N-terminal part of various BLUF domains. The conserved tyrosine and the mutated position 31 are shown in boldface type. From the dark-adapted state structure of the WT (*B*), the predominant interactions of the flavin cofactor with the protein are hydrogen bonds from Gln-50 to N5, a hydrogen bond from Asn-31 to C2=O, and hydrogen bonds between N3, C4=O, and Asn-32. Homology models (*C*) of the N31R (*orange*) and N31H (*green*) mutants show the putative positive charge of these mutated side chains near the C2=O carbonyl group. Furthermore, the residues are interacting with the negatively charged phosphate group of the flavin cofactor, supporting its coordination by Arg-30.

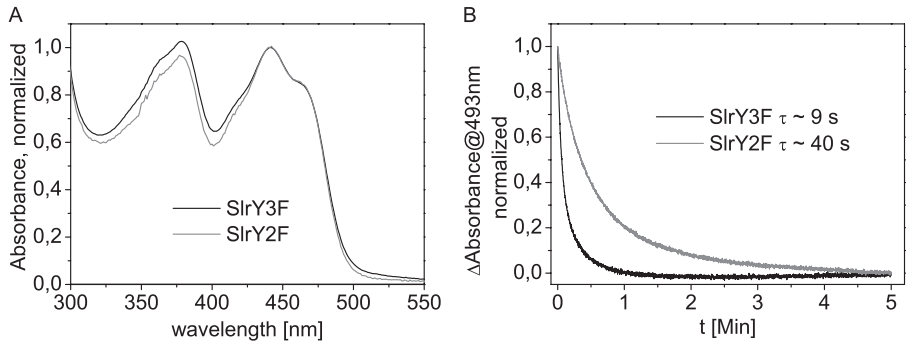

FIGURE 2. **Absorption and dark state recovery of SlrY2F (*gray*) and SlrY3F (*black*).** The dark-adapted spectra of the fluorotyrosine-substituted Slr1694 BLUF domains (*A*) are highly similar with absorption maxima of the S_0-S_1 transition at 441 nm identical to the WT. Minor differences are visible due to slight scattering of the SlrY3F protein indicated by an apparent increase in absorption toward shorter wavelengths. Dark recovery at room temperature after illumination at 450 nm was monitored at 493 nm (*B*). The time constants of the process are about 9 s for SlrY3F and 40 s for SlrY2F.

to measure SlrY3F in D_2O buffer, which has a sufficiently fast dark recovery under these conditions. Because of their decreased dark recovery rate (see above), the remaining samples do not allow for a complete recovery in the described experimental setting, which would lead to a mixing of dark- and light-adapted states. Because of their spectral similarity, both states would then be excited by the pump beam, and a mix of spectral dynamics would be observed.

The main interest of this study is the first step in photoactivation of BLUF domains, which is photoinduced electron transfer. This process can be conveniently monitored at around 700 nm (Fig. 3). At this wavelength, only the excited state of flavin absorbs significantly without contributions of anionic or neutral flavin semiquinones that are expected to form as observed previously (13, 36, 44). A loss of absorbance at this wavelength therefore corresponds to excited state deactivation processes,

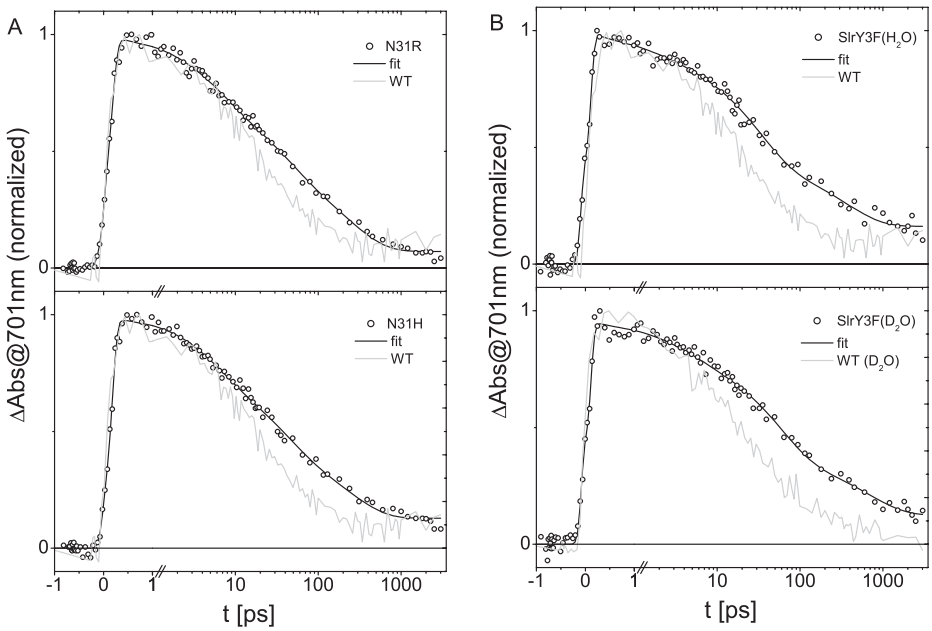

FIGURE 3. **Excited state decay of the flavin in Slr1694 and mutants.** The absorbance change at 701 nm is characteristic for excited state decay of the flavin. Slr1694-N31R/N31H (*A*, *black*) show a significantly slower decay than the WT (*gray*), especially at delays greater than 10 ps. SlrY3F in both H_2O and D_2O shows an even slower excited state decay (*B*).

which are dominated by photoinduced electron transfer in BLUF domains. In Fig. 3, the corresponding traces are depicted along with the absorbance change of the WT protein at this wavelength (adapted from data presented by Gauden *et al.* (13)). All proteins show a clearly elongated excited state lifetime of the flavin. The excited state decay of all mutants and Slr-Y3F is similar to the wild type within the first 3 ps, for the Asn-31 mutants even within the first 6 ps. Afterward, the decay clearly deviates from the wild type. Among these proteins, SlrY3F in both D_2O and H_2O shows the longest excited state lifetime. SlrY2F showed very similar photodynamics to SlrY3F on the ultrafast time scale (not shown) and is therefore not discussed here.

Spectral Evolution—To obtain an overall picture of the spectral evolution and to assess whether reaction intermediates can be observed in the obtained data sets, we first analyzed the data globally using a sequential model with increasing lifetimes ($1 \rightarrow 2 \rightarrow 3 \rightarrow 4 \ldots$). The corresponding evolution-associated difference spectra (EADS) are displayed in Fig. 4. The following applies to all data sets. The first spectra (*black*) correspond purely to the singlet excited state of the flavin that is formed during the instrument response. The main components of these spectra typically are the ground state bleach (GSB) around 445 nm, excited state absorption (ESA) around 510 nm and above 600 nm, and stimulated emission (SE) at around 550 nm. The final, non-decaying spectra correspond to a species that does not decay on the time scale of the experiment and is predominantly assigned to the difference spectrum of the signaling state of the BLUF domain, as indicated by the dark state bleach around 445 nm and the red-shifted absorption at around 490 nm. In all cases, a featureless absorption from 500 to 700 nm is observed in varying amounts, which is attributed to flavin triplet absorption (37). The spectral evolution from the black to the final spectra will be described for all studied BLUF domains as follows.

The Slr1694-N31R and N31H mutants behave similarly in their spectral evolution and are both sufficiently described using five lifetimes (Fig. 4, *A* and *B*). The red EADS is formed from the black in roughly 1 ps (N31H) and 1.2 ps (N31R) along with a significant blue shift and increase of the SE band from about 560 to 550 nm, which is indicative of vibrational relaxation in the flavin excited state (13, 36, 37, 44). The red EADS then decays in 5.1 ps (N31H) and 5.5 ps (N31R) into the green EADS with a loss and further blue shift of the SE band. Additionally, the green EADS gain absorption between 570 and 620 nm, which indicates the formation of a flavin semiquinone species, as observed previously (13, 44). Its rise and decay are indicated at single wavelength traces around 600 nm (supplemental Fig. S1). At the same time, ESA above 620 nm is diminished by about 25%. From the green EADS, the blue EADS is formed in 36 ps (N31H) and 37 ps (N31R), which is characterized by a loss of GSB of about 50% and a complete (N31H) or almost complete (N31R) loss of SE. Additionally, a shoulder in the positive absorption at around 490 nm is formed, along with a further increase in absorption between 550 and 600 nm. The final magenta EADS is formed in about 240 ps in both mutants with a quantum yield of about 32% (N31H) and 29% (N31R), as judged from the induced absorption at 490 nm relative to the GSB in the very first spectrum compared with previous experiments (44). The N31H data set seems to contain about 2 times more flavin triplet species than N31R, as judged by the broad absorption near 650 nm.

The spectral evolution of SlrY3F (Fig. 4, *C* and *D*) and SlrY2F (not shown) is highly similar. We will therefore focus only on the description of the SlrY3F sample. Similar to the spectra of the Asn-31 mutants, the red EADS is formed from the black in 1 ps with an increase and a slight blue shift of SE. The red EADS then evolves into the green with 2.7 and 4.3 ps (D_2O). The green EADS shows a significant blue shift of the SE band. Additionally, the ESA feature at around 510 nm becomes narrower and

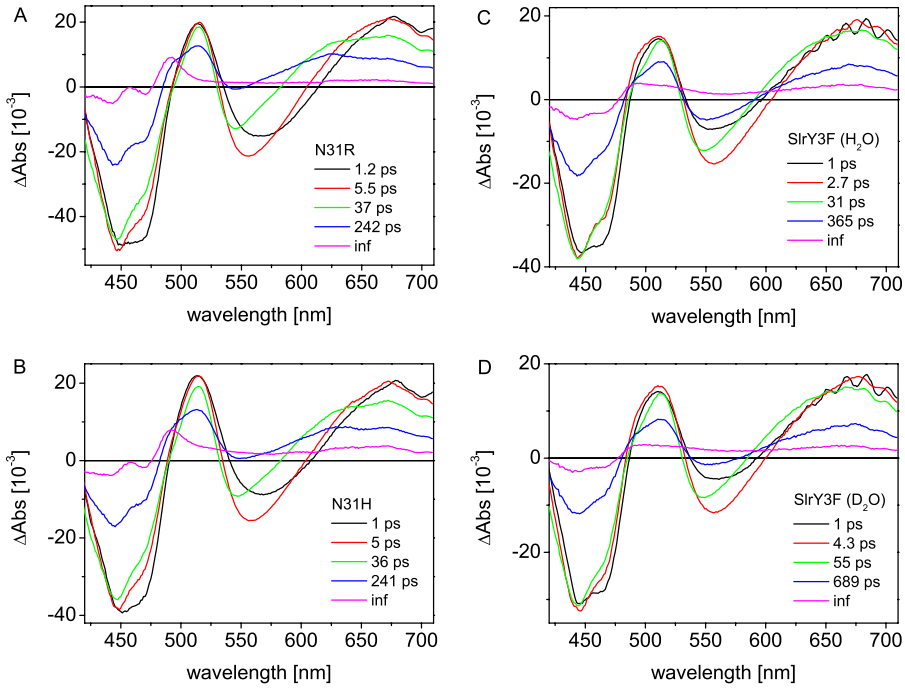

FIGURE 4. **Spectral evolution of Slr1694-N31R (*A*), Slr1694-N31H (*B*), and SlrY3F in H_2O (*C*) and D_2O (*D*).** The EADS show the spectral evolution after femtosecond excitation. The spectra evolve sequentially with the indicated lifetimes (*black* → *red* → *green* → *blue* → *magenta*).

shows a shoulder at around 490 nm. Similar to the spectral evolution of the N31R and N31H mutants, some absorption between 580 and 600 nm rises (see also supplemental Fig. S2), but to a significantly smaller degree, whereas ESA above 625 nm remains unchanged. The green EADS evolves into the blue spectrum with a lifetime of 31 and 55 ps (D_2O) with a ~50% loss of GSB and ESA. SE is also diminished but still clearly present. The blue EADS then evolves in 365 and 689 ps (D_2O) into the non-decaying species. Compared with the data set of the N31R mutant, the final spectrum of the SlrY3F data sets shows a larger amount of featureless absorption between 500 and 700 nm. The apparent broadening of the induced absorption at 490 nm, which is indicative of the BLUF signaling state, is due to spectral overlap with triplet absorption. As judged from the absorption at 650 nm, the SlrY3F protein yields similar amounts of triplet in H_2O and D_2O, similar to the N31H mutant. The quantum yield of signaling state formation estimated as above is significantly lower than for the Asn-31 mutants with about 16%.

Target Analysis of the N31R and N31H Mutants—In the past, target analysis proved to be a powerful tool to reveal the ultrafast photochemistry of BLUF domains (13–15, 36, 37, 43, 44). By fitting transient data using branched compartmental models, parallel reaction pathways can be investigated, and inverted kinetics, where a product is decaying faster than its formation, can be addressed. The resulting so-called species-associated difference spectra (SADS) ideally represent the difference spectra of the true molecular species that occur during the reaction. Using this approach on transient absorption data of Slr1694, the presence of an anionic and a neutral semiquinone flavin radical was demonstrated previously (13, 14). Due to the strong multiexponentiality of the excited state decay in BLUF domains ranging from a few ps to hundreds of ps, the electron transfer from a nearby tyrosine and the resulting anionic flavin radical product, which occur in a few ps, are difficult to observe directly. Additionally, the subsequent protonation of the anionic flavin radical also occurs in only a few ps. Because also the protonated semiquinone lives only for tens of ps, either intermediate is difficult to resolve kinetically. A multiexponential excited state decay, as previously observed for BLUF domains (13, 14, 36, 44), is clearly visible in the transient absorption at 701 nm (Fig. 3). To obtain spectra of the pure intermediate states, we applied target analysis taking this behavior into account. Additionally, we considered vibrationally hot excited state relaxation because it was indicated by the blue shift of stimulated emission observed in the sequential analysis above. Finally, a non-decaying species is assumed for the red-shifted signaling state $BLUF_{red}$, which however may be mixed with triplet features that are not expected to decay on the time scale of the experiment and are therefore impossible to separate from each other. In the model for the N31H mutants (Fig. 5*A*), two intermediates (Q1 and Q2) formed sequentially from the multiexponential excited state decay were included, identical to the model for the WT (13, 44). SlrY3F, however, was best described with only one intermediate (Q1) in both H_2O and D_2O (Fig. 5*A*) and is therefore discussed separately. Similar to WT, we also included a 50% loss after the Q1 intermediate, ascribed to radical recombination prior to proton transfer (13).

To get a better handle for discussion of the obviously slowed down excited state decay rates, as already observed in the raw data (Fig. 3), we describe this multiexponential process in the following by averaged lifetimes calculated as follows,

$$k_{avg} = e^{\sum_n \ln(k_n) \times f_n} \quad \text{(Eq. 1)}$$

where k_n represent the respective decay rates, and f_n are the corresponding fractions obtained by target analysis. The life-

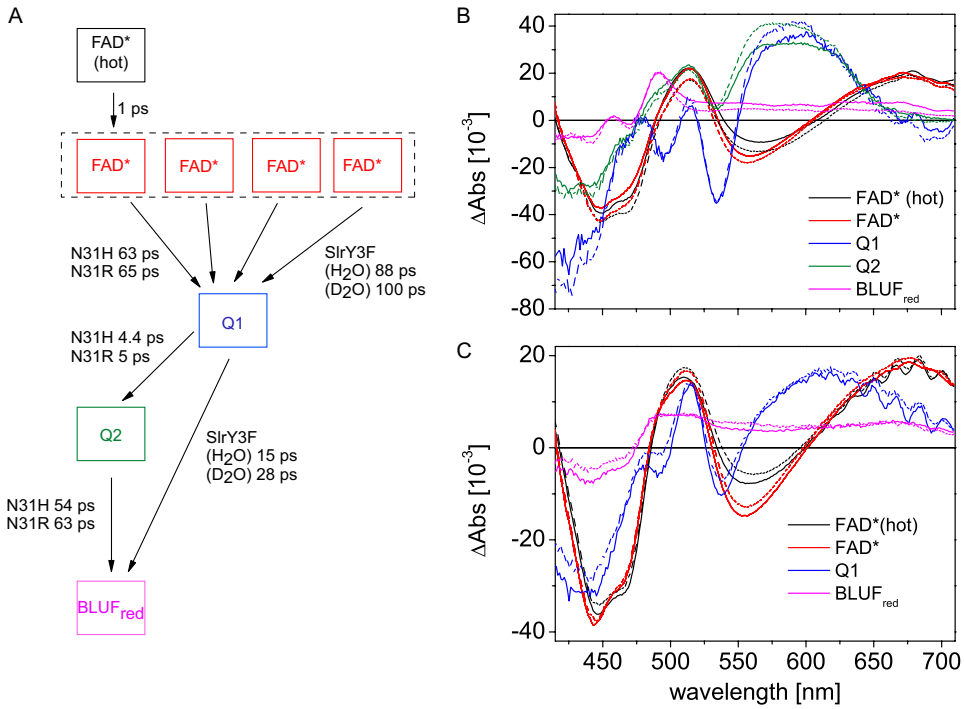

FIGURE 5. **Target analysis of Asn-31 mutants of Slr1694 (*A* and *B*) and Slr1694 substituted with 3-fluorotyrosine SlrY3F (*A* and *C*).** The model used for the description of both N31H (*B*, *solid lines*) and N31R (*B*, *dashed lines*) is displayed in *A* together with the average lifetimes for the multiexponential reaction from the FAD* excited state (*red*) to Q1 (*blue*). The model used for the description of SlrY3F in both H_2O (*C*, *solid lines*) and D_2O (*C*, *dashed lines*) data sets is similar to the N31H/R model (*A*) except that the reaction proceeds from Q1 directly to the red-shifted state ($BLUF_{red}$).

times and their corresponding fractions obtained from the target analysis below are displayed in Table 3. The average lifetimes (τ_{avg}) displayed in Table 3 and Fig. 5*A* are the reciprocal values of k_{avg}. The logarithmic way of weight averaging the rates provides a more unbiased average than weight averaging either the lifetimes or the decay rates directly, because using the lifetimes will put more weight on the bigger lifetimes, whereas using the rates will emphasize the shorter lifetimes/bigger rates.

The data sets of the Asn-31 mutants were best fitted with a model identical to the WT as shown in Fig. 5*A* and gave qualitatively identical spectra for both mutants (Fig. 5*B*). This model includes two intermediates (Q1 and Q2). The hot (black) and relaxed (red) excited state SADS represent flavin excited states with GSB around 445 nm, ESA absorption at 510 and above 600 nm, and stimulated emission around 550 nm. The relaxed state is formed in 1 ps in both mutants and characterized by a blue-shifted SE band. The decay of the relaxed excited state into the Q1 intermediate was described best using four lifetimes. The lifetimes differ only slightly between the two data sets (Fig. 5*A*). Compared with the wild type (Table 3), the average lifetime is slowed down to 63 and 65 ps (WT, 17 ps) due to lower fractions of the fast components and the presence of clearly elongated lifetimes with significant contributions.

The Q1 intermediates in the N31H and N31R mutants significantly differ in their spectral properties from the Q1 intermediate detected in WT. The spectrum is characterized by the same induced absorption above 550 nm, which is characteristic for an anionic semiquinone species with charge transfer (CT) character (57). Strikingly, the Q1 SADS shows a negative band at 525 nm. Negative bands in transient absorption spectroscopy are assigned either to GSB or SE, and given that there is no ground state absorption at 525 nm, the negative feature must be assigned to SE. Thus, we conclude that this species, at least partly, corresponds to a flavin excited state. At first glance, one may interpret the Q1 SADS as a WT Q1 spectrum that is "contaminated" by FAD*. However, this can be ruled out because the negative feature at 525 nm has a spectral shape that differs significantly from that of FAD*. Additionally, the spectral evolution of N31H clearly indicates the formation of a shifted SE feature in contrast to WT (supplemental Fig. S3). A target model without this intermediate led to a significantly worse fit in this time domain (not shown), which proves that inclusion of an emission component in Q1 is strictly required.

The Q1 intermediates decay into the next intermediate (Q2) with WT-like lifetimes of 4.4 ps (N31H) and 5 ps (N31R). The Q2 intermediate nicely represents a neutral semiquinone flavin radical, which is characterized by the complete absence of SE and a broad absorbance between 550 and 650 nm. Similar to WT, we observe a significant loss in GSB in both data sets (13, 14, 44) if the 50% loss mentioned above is not included. This loss is believed to originate from radical recombination of the anionic flavin semiquinone and tyrosyl cation, thus preventing quantitative formation of the neutral semiquinone. The Q2 intermediates decay with 54 ps (N31H) and 63 ps (N31R) into the final non-decaying spectrum. This values are in close range of the 65 ps observed for the neutral flavin semiquinone in WT (13). The final non-decaying spectrum is identical to the one obtained from global analysis and shows the characteristic induced absorption of the red-shifted signaling state at around 490 nm and a broad featureless absorption most likely corresponding to a flavin triplet.

TABLE 3

Excited state decay lifetimes (τ) of various BLUF domains, their fractional contributions, and the corresponding weighted average lifetimes (τ_{avg})

The last row shows the quantum yield of signaling state formation (Φ_{red}).

	Slr1694 WT (13)	Slr1694-N31H	Slr1694-N31R	SlrY3F	SlrY3F (D_2O)	AppA (37)	BlrB (36)
τ (ps)	7 (47%)	6.7 (20.6%)	6.9 (20.6%)	2.8 (7.3%)	2.8 (7.3%)	90 (38%)	18 (27%)
	40 (28%)	37 (34.6%)	43 (34.6%)	11.5 (26.6%)	11.5 (26.6%)	570 (59%)	216 (73%)
	180 (17%)	179 (38.2%)	181 (38.2%)	101 (34.5%)	111 (34.5%)	1000 (3%)	
	209 (0.1%)	3448 (6.6%)	1667 (6.6%)	943 (31.5%)	1266 (31.5%)		
τ_{avg} (ps)	17	63	65	88	100	287	110
Φ_{red}	40%	33%	29%	16.5%	15%	24%	30–40%

Target Analysis of the SlrY3F Protein—For the fluorotyrosine-substituted protein, we extracted an intermediate, which is strikingly similar to the Q1 spectrum of the Asn-31 mutants, varying slightly by an increased absorbance above 650 nm and at 510 nm. The model (Fig. 5*A*) again features hot state (*black*) cooling into the relaxed excited state (*red*) and formation of the non-decaying species (*magenta*) via the Q1 intermediate (*blue*; Fig. 5*C*) without any further intermediate. Similar to the Asn-31 mutants, the excited state spectra perfectly match flavin excited state features with a blue shift of the SE band during the 1-ps hot state relaxation. The excited state decay into the Q1 intermediate was described best using four excited state lifetimes with varying concentrations (Fig. 5*A* and Table 3). The kinetic isotope effect on the slower components is small (1.1–1.3) and is not further interpreted. Compared with WT and the Asn-31 mutants (Table 3), the average lifetime is slowed down further to 88 ps (100 ps in D_2O) due to the dominating contributions of the slow components in the nanosecond time scale. The semiquinone characteristics of the Q1 intermediate at around 600 nm are clearly observed in kinetic traces around this wavelength (supplemental Fig. S2) and support the global fitting procedure. The decay of the Q1 intermediate at 600 nm also shows a clear kinetic isotope effect of about 1.9, which is supported by the raw data (supplemental Fig. S2). The final spectra in both data sets are very similar and resemble the red-shifted signaling state together with contributions of rather featureless absorption between 500 and 700 nm assigned to flavin triplets.

Spectral Fitting of the Q1 Intermediate—The Q1 spectrum observed here is clearly distinguished from the Q1 intermediate observed in the WT (13) and W91F (44) mutant by pronounced additional negative features at ~510 and 540 nm, which indicate a stimulated emission contribution in this species. This observation implies that this SADS represents a fraction of flavins in an excited state. To identify the nature of the Q1 intermediate, we reconstructed the difference spectrum by spectral fitting of a linear combination of experimentally known contributions and spectral characteristics of excited state absorption and stimulated emission of flavins in BLUF domains. We used experimentally determined spectra of the ground state absorbance to describe the GSB and skewed Gaussians to describe stimulated emission and (excited state) absorbance (Fig. 6). In Fig. 6, a comparison of spectral fits of the Q1 intermediate of N31H, N31R (Fig. 6, *A* and *B*), SlrY3F (Fig. 6, *C* and *D*), and WT (Fig. 6, *E* and *F*), the latter two in H_2O and D_2O, is displayed. In WT, the Q1 spectrum is sufficiently described using the ground state bleach (*green*) and three skewed Gaussians (*blue*, *red*, and *magenta*) for the absorption of the intermediate in H_2O and D_2O. In the modified proteins, an additional Gaussian (*black*) at around 525 nm was necessary to account for the negative contributions at 500 nm and 540 nm. This additional contribution at ~525 nm can only originate from stimulated emission, demonstrating that Q1 corresponds at least partly to an excited state species. In supplemental Fig. S4, we present a fit of all photocycle intermediates for the N31H mutant, with known contributions from ground state bleach, stimulated emission, and red-shifted product absorption imposed in the fit. The FAD* species shows stimulated emission from the excited state to the ground state, peaking at ~510 nm, as follows from the fluorescence spectrum, whereas Q2 and the final product are devoid of any stimulated emission. The SE observed in the Q1 intermediate is therefore present only in this intermediate and red-shifted compared with the locally excited state FAD*. A red shift in fluorescence/SE may be indicative for the formation of a CT state.

DISCUSSION

Up to now, only a few BLUF domains were studied with regard to the primary photochemistry. Therefore, the primary mechanisms that facilitate formation of the biological signaling state and determine most likely also biologically relevant parameters like photosensitivity (quantum yield of signaling state formation) are still not fully understood. Although the BLUF domains share a very similar amino acid composition of their flavin binding pocket, the differences in excited state lifetimes ranging from about a few ps in Slr1694 (13) to hundreds of ps in AppA (37) have not been addressed on a molecular level. In this study, we observed how the redox potential of the tyrosine/flavin reaction pair, which constitutes the first step in BLUF photoactivation, determines excited state lifetime as well as photoproduct quantum yield.

Observation of an Excited State Charge Transfer State in BLUF Domains—The elongated excited state lifetimes in the Asn-31 mutants and SlrY3F provided us with further insight into the BLUF photocycle by revealing a hitherto unobserved excited state. In both Asn-31 mutants and SlrY3F, we found the presence of an intermediate (Q1), which features the previously observed charge transfer absorption of the anionic flavin semiquinone but additionally shows stimulated emission features indicative of an excited state species. By spectral fitting of the Q1 intermediates observed here and the Q1 intermediates observed in WT before, we clearly assign the difference to stimulated emission that is red-shifted to ~525 nm compared with that of the locally excited state FAD*. Therefore, we believe that the Q1 intermediate indicates the presence of an excited state with strong charge transfer character, which

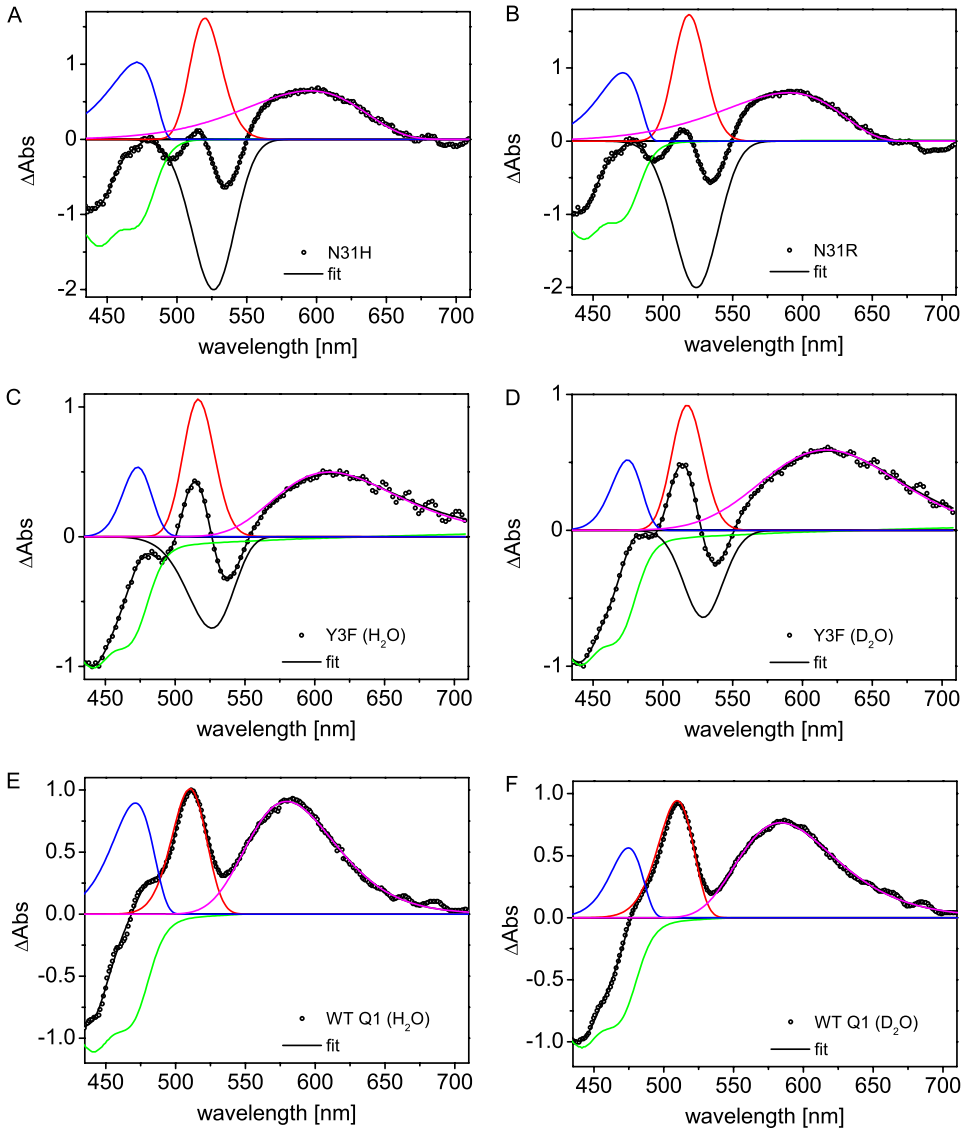

FIGURE 6. **Spectral fits of the Q1 intermediates of the Asn-31 mutants (*A* and *B*) and SlrY3F (*C* and *D*) compared with WT (*E* and *F*) using experimentally determined ground state absorbance (*green*) and skewed Gaussians for (excited state) absorption (*blue*, *red*, and *magenta*) and stimulated emission (*black*).**

is formed from the locally excited state (FAD*) prior to full electron transfer (Fig. 7*A*). Interestingly, fluorescence depolarization experiments in glutathione reductase provided evidence for an emissive flavin/tyrosine CT state with a shifted emission dipole moment decaying in the same time domain (58). Hence, we hypothesize that the excited CT state observed here most likely corresponds to significant electron redistribution from Tyr-8 to FAD in the excited state.

The Q1 intermediate in the Asn-31 mutants has a spectral signature of the anionic $FAD^{\bullet-}$ CT absorption band near 600 nm that is very similar to that of WT. Moreover, its lifetime of ~5 ps is essentially the same as in WT. Therefore, it is likely that the Q1 species is not a single molecular species but that it represents a mixture of an excited CT state with the anionic semiquinone $FAD^{\bullet-}$. Such a mixture may appear in the case of heterogeneity in the initial reaction rates, which in a fraction of the BLUF domains results in transient accumulation of the excited CT state and in the remaining fraction in transient accumulation of the $FAD^{\bullet-}$ species.

The question arises whether the proposed FAD*/Tyr excited CT state forms an integral part of the photoreaction in WT BLUF or if this species is a characteristic feature of the modified BLUF proteins only. Given that functionally the photoreactions in N31R and N31H are the same as in WT, it is very likely that in WT, the reaction proceeds via such a species as well but that it cannot be kinetically resolved due to a rate-limiting formation rate. We therefore propose that the FAD*/Tyr excited CT state generally applies to the BLUF photoreaction and that it becomes observable in the N31R/H mutants and Slr-Y3F protein through their modified reaction rates.

The Q1 species is subsequently protonated to the neutral semiquinone. In case of the Asn-31 mutants, one can safely assume that the proton transfer reaction from the tyrosine remains largely unaffected, which is indicated by the virtually identical rise time and lifetime of the neutral flavin semiquinone (Q2) in the WT.

The Q1 spectrum of SlrY3F is highly similar to the Q1 intermediate in the Asn-31 mutants and therefore considered to be

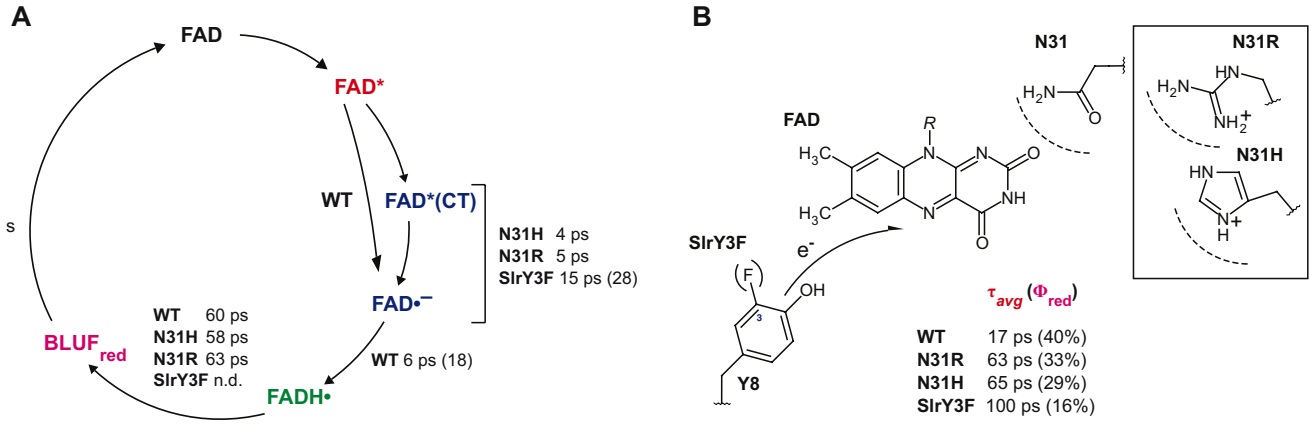

FIGURE 7. *A*, in the Slr1694 Asn-31 mutants and modified proteins, the slowed down excited state decay leads to an accumulation of a charge transfer state FAD*CT formed from the locally excited state FAD* prior to formation of the anionic semiquinone ($FAD^{\bullet-}$), which appears to be formed instantly in WT. The lifetimes in the modified proteins correspond to a mixture of CT and anionic radical species. In the Asn-31 mutants, the subsequently formed neutral flavin semiquinone ($FADH^{\bullet}$) decays to the red-shifted state with similar lifetimes as the WT. In SlrY3F, this intermediate cannot be observed, and the red-shifted state appears to be formed directly from the FAD*CT/$FAD^{\bullet-}$. The average excited state lifetime (τ_{avg}), which corresponds to excited state electron transfer between tyrosine and flavin in BLUF domains (*B*), is slowed down by modification of the electron donor (SlrY3F) or a positive charge near the C2=O carbonyl of the acceptor (N31R and N31H). Additionally, the quantum yield of signaling state formation (Φ_{red}) becomes lower with increasing excited state lifetime.

of almost identical nature. The decay of this species is slowed down 3-fold compared with WT Q1 and shows a clear kinetic isotope effect of 1.9. Due to the higher acidity of the hydroxyl group of the fluorinated tyrosine (59), one would assume that the proton transfer to the flavin is even faster than in WT and the value obtained here by global fitting. This would then lead to an accumulation of the neutral radical form, which is apparently not the case. Thereby, the subsequent radical recombination step, which involves proton-coupled electron transfer to form the red-shifted state apparently occurs in the same time domain as its formation. Compared with WT, this reaction is accelerated here, which is reasonable because the fluorination renders the tyrosine radical in an energetically less favorable redox state. Small contributions from a neutral semiquinone mixed with the CT and anionic semiquinone spectrum might account for the increased absorbance at 510 nm in SlrY3F Q1 compared with N31H/R-Q1 (Fig. 6), which was previously observed to be higher in the neutral semiquinone than in the anionic form (13).

With these new experimental insights at hand, we propose a more detailed photocycle scheme for BLUF domains (Fig. 7*A*). After excitation of the flavin, significant charge redistribution from tyrosine to flavin takes place before the complete electron transfer is accomplished. In Slr1694 WT, electron transfer is too fast to kinetically resolve this excited state FAD*/Tyr CT intermediate and seems to directly proceed to the ground state anionic flavin semiquinone. In Slr1694 proteins with slowed down electron transfer properties, this intermediate becomes partly detectable in transient absorption spectroscopy by its red-shifted SE contribution. Because of its otherwise spectral and kinetic similarity to the WT flavin anionic semiquinone species, it is most likely that we observe a mixture of excited FAD*/Tyr CT state and flavin anionic semiquinone/tyrosyl radical pair.

Positive Charges Close to the Flavin C2 Carbonyl Slow Down Electron Transfer in Slr1694—Besides distance, orientation, and reorganization energy, the relative redox potentials in a given reaction partner system are of major influence for the free reaction energy and thereby also for electron transfer rates. The redox potential of a molecule can be influenced indirectly by changes in the environment (*e.g.* polarity and dielectric constant) or by subtle chemical modifications of the molecule itself. In a biological context, redox processes are evolutionarily optimized and present the best fitting environment for the corresponding task. The redox potential of flavin is known to be strongly influenced by positive charges close to the C2 carbonyl of the flavin, which has been observed previously in many flavoenzymes (60, 61). The positive charge close to this part of the flavin is thought to stabilize negatively charged flavins because the charge density in flavins is generally more localized on the heteroatom-rich part of the isoalloxazine moiety, especially in the excited state or in charge transfer states. So far, redox potentials of flavin in BLUF domains have been experimentally addressed only for AppA and several mutants thereof (62). The redox potential for the ground state of the FAD/FAD^{-} redox pair in the WT BLUF domain was determined to be about −260 mV (*versus* SCE), about 50 mV lower than for FAD in solution. Interestingly, BLUF domains are highly variable in their amino acid composition close to the C2 carbonyl (Fig. 1*A*). Slr1694, which so far shows the fastest excited state decay (Table 3) and therefore also the fastest photoinduced electron transfer, contains a polar but uncharged asparagine at position 31 (Fig. 1, *A* and *B*). BlrB and AppA, which show a slightly and significantly slower photoinduced electron transfer, respectively, contain an arginine or a histidine at the corresponding position (36, 37). Both side chains are supposed to be positively charged in the protein under the experimental conditions applied here. The protonation state of His-44 in AppA was previously confirmed by NMR spectroscopy (63). Assuming that these positive charges stabilize also a singly reduced flavin, one would expect an increase in the FAD/$FAD^{\bullet-}$ redox potential and thereby a corresponding increase in free reaction energy. In contrast, a significantly

slowed down photoinduced electron transfer is observed for these WT proteins and the Slr1694-N31R/H mutants (Fig. 7*B* and Table 3). If we consider the overall protein configurations and especially the mutual distance and orientation of flavin and tyrosine identical to that in the WT protein, this putatively redox potential-induced change in reactivity may be explained by the Marcus theory (64–66). The increase in free energy by elevating the redox potential of the flavin might push the reaction into the so-called inverted region. In this region, an activation barrier appears, which then slows down the reaction itself but still yields a higher free energy. Generally, the reorganization energy for complex systems like proteins is very high, and therefore it is usually hard to reach the inverted regime. Here, however, we are looking at an excited state reaction, which most likely provides sufficient energy; the redox potential in the singlet excited state of flavin is elevated enormously by ~1 V (67). Additionally, Marcus inverted regions have also been found in ET reactions of photosynthetic reaction centers (68) and have been recently observed for the back electron transfer reactions to the neutral flavin semiquinone in DNA photolyase after DNA repair as well (69).

It should be noted that although we observe a significant effect on the ET rates, the redox potential of the one-electron reduction of flavin might be shifted only slightly. In a previous theoretical study on flavodoxins, a shift of 20 mV was calculated for mutants, where charged or polar side chains were introduced close to the flavin (45).

The average excited state lifetimes of N31H/R with 63 and 65 ps, respectively, are significantly slower than in WT (17 ps) but still clearly faster than BlrB with 110 ps or AppA with 287 ps. Interestingly, mutated AppA-H44R, which turns AppA into a BlrB-like protein with respect to the C2=O environment, leads to a significant speeding up of the primary reaction (39). In Slr1694, we are obviously not able to discriminate the AppA-like mutation N31H and the BlrB-like mutation N31R because the difference in the excited state lifetimes of all fractions is only marginal (Table 3).

Redox Modulation of the Electron-donating Tyrosine in Slr1694—In tuning the redox properties of the BLUF domain, we also applied a different approach directly affecting the tyrosine redox partner, which is a well known procedure for modifying and investigating PCET in photosynthesis research (33). In this study, we used a procedure in which a tyrosine analog, fluorotyrosine, is incorporated selectively into the protein *in vivo* using a tyrosine biosynthesis-deficient *E. coli* expression strain. A similar procedure was previously employed to modify the GFP chromophore (70). Here we decided to design a novel tyrosine-deficient *E. coli* expression strain using CmpX13 (47), a C41(DE3) (71) derivative with constitutive expression of a riboflavin transporter, as a parent strain. This strategy is advantageous for the production of flavoproteins under the conditions encountered here. For selective labeling, the cells have to be cultivated in defined/minimal medium, which is usually not optimal for cell vitality. Additionally fluorinated tyrosine, which is present during protein production, is also incorporated into household proteins of the cell and might thereby impair their function. Both conditions might also lead to a lack or even a breakdown of cofactor biosynthesis, which is easily circumvented by external supplementation of riboflavin in the medium. In our experiments, we indeed observed a lower vitality of the expression culture, indicated by the lowered biomass yield.

The introduction of a fluorine atom at the tyrosine ring resulted in a functional, photoactivatable BLUF protein. This chemical modification not only increases the redox potential from 650 to 700 mV (*versus* NHE) of the $Tyr^{\bullet}/Tyr^{-}$ redox pair but also lowers the pK_a of the phenolic group by more than 1 order of magnitude to about 8.4, thus increasing its acidity (59). Additionally, one should take into account that although the fluorine atom is very compact and the substitution can be considered by and large isosteric, the fluorine substitution inverses the polarity of the former C–H bond and may therefore also act as a hydrogen bond acceptor and establish new interactions within the protein (72). Because the protein still binds flavin similar to the WT protein and the dark-adapted state absorbance and also the dark recovery in at least the SlrY3F protein remains unchanged, one can assume that the flavin binding pocket is not significantly distorted by this tyrosine analog. The increased redox potential of the fluorinated tyrosine stabilizes its reduced form and is thus expected to transfer its electron to the excited state flavin more slowly, as indeed is observed here. It is also noteworthy that in AppA, the redox potential of the flavin is largely unaffected by the substitution of tyrosine by phenylalanine, which suggests that we can safely assume that only the redox potential of the tyrosine and not the redox potential of the flavin is changed by this modification (62). The average excited state lifetime (Table 3) of 88 ps (100 ps in D_2O) is clearly longer than for the Asn-31 mutants and close to the BlrB average lifetime (110 ps/120 ps in D_2O (36)). The effect of changes in the redox potential of the tyrosine on the photoinduced electron transfer therefore appears larger than the indirect effect of the environment of the flavin C2=O carbonyl. The environment of the reactive tyrosine in BLUF domains, however, has not been studied so far. From our experience, mutagenesis close to this tyrosine is generally difficult to accomplish without disturbing the protein fold.[5]

Studies on the environment of Tyr-8 would be highly interesting because another influence for the redox potential of Tyr-8 may be the nature of hydrogen bonding to the conserved Gln-50 side chain amide. In a theoretical study by Ishikita (46) on the ET driving force in light- and dark-adapted states of the AppA BLUF domain, the redox potential of the tyrosine seemed to be influenced significantly by the side chain orientation of the conserved glutamine, whereas the flavin remained largely unaffected. The ET driving force would thereby be significantly enhanced for the light state, which is consistent with the results of Toh *et al.* (73), who observed a dramatically increased electron transfer rate in the light state. It is difficult, however, to directly relate the results on AppA to the Slr1694 BLUF domain because photoinduced ET rates are much faster in the latter protein (17 ps *versus* 287 ps; see Table 3). In fact, in TePixD, which is highly homologous to Slr1694, ET in the dark-adapted state was found to occur at optimal ΔG on the top of the Marcus curve (42). The ET rate of the dark-adapted AppA is signifi-

[5] T. Mathes, I. H. M. van Stokkum, M. Stierl, and J. T. M. Kennis, unpublished observation.

cantly slower and may be far off the maximum of the Marcus curve accordingly. Therefore, the enhanced ET rate in Slr1694 in the light state (which occurs very rapidly in 1 ps (15)) is most likely due to other factors like shortened Tyr/FAD distance or optimized MO overlap.

Because the change of the redox potential of the tyrosine and flavin leads to a lower or higher free reaction energy, respectively, and ET is slowed down in both cases, ET in WT Slr1694 must be optimized almost perfectly and occur in an almost barrier-less manner according to the Marcus theory. A similar proposal has been made by Shibata *et al.* (42), who studied the highly homologous TePixD BLUF protein by time-resolved fluorescence spectroscopy.

Previously, we modulated the tyrosine redox partner by exchanging the phenolic side chain by an indole moiety using site-directed mutagenesis (44, 74). Although the Slr1694-Y8W mutant was able to photoreduce the flavin to a radical state with high efficiency, no signaling state was formed, probably due to alterations in the flavin-coordinating hydrogen bond network involving Gln-50. The light-induced reaction produced various spectrally distinct radical pair difference spectra on the ultrafast time scale, which were assigned to FAD/Trp-8 radical pairs but might also correspond to a radical pair consisting of FAD and the semiconserved Trp-91. Using transient EPR spectroscopy, a strongly coupled radical pair was detected in this mutant, which was significantly different from the WT radical pair and decayed slightly slower (74). Because the Y8W mutation, however, rendered the BLUF photoreceptor non-functional and the radical pairs probably originate from the FAD triplet state rather than the singlet excited state, these findings are difficult to relate to WT and functional BLUF mutants directly.

The Quantum Yield of Signaling State Formation Is Affected by Redox Modulation of FAD/Tyr—An interesting aspect of this study is the obvious decrease of the quantum yield of signaling state formation along with the elongation of excited state lifetime (Table 3 and Fig. 7*B*). In Slr1694, which shows the fastest excited state decay, we observe a quantum yield of roughly 40%, and in BlrB the quantum yield ranges between 30 and 40% (36, 75) as compared with about 24% AppA (37), which has the slowest ET reaction observed in BLUF domains so far. In AppA, the quantum yield can be increased to about 30% by introducing the BlrB-like H44R mutation (39), analogous to the Slr1694-N31R mutation. Additionally, an increase up to 37% can be achieved by removal of a semiconserved tryptophan side chain that competes in the excited state electron transfer with the tyrosine but only yields a futile reaction that does not contribute to signaling state formation (43). Because this competing process was not observed in Slr1694, which is probably due to a larger distance of this tryptophan from the flavin as compared with AppA (44), we also do not consider it in the Slr1694 variants investigated here. However, due to the significantly elongated lifetime of the flavin excited state, we cannot exclude competing ET from Trp-91 completely. The quantum yield in the modified Slr1694 proteins drops as a result of changes in the redox potential from 40% in the WT to ~30% in both Asn-31 mutants with clearly elongated average excited state lifetimes of about 65 ps down to ~16% in the fluorotyrosine-substituted protein with an even longer average excited state lifetime of about 100 ps.

This correlation is also of interest for the question regarding which step in the photocycle promotes the putative rotation of the Gln-50 side chain amide and therefore constitutes a prerequisite for the signaling state. Ishikita (46) reported calculations on the AppA BLUF domain in putative light and dark state conformations, which suggested that the light-induced charge separation forms the main driving force for the rotation. Generally, this would be in line with our finding here that a decreased ET rate correlates with a lowered signaling state quantum yield. However, the lowered signaling state quantum yield might well be due to various loss processes in the photocycle like an overall reduced quantum yield of the light-induced ET reaction or an enhanced radical pair recombination of $Y^{\bullet+}/FAD^{\bullet-}$. Both would contribute to a loss in the subsequent proton transfer to form $FADH^{\bullet}$, which we previously suggested to be a trigger for Gln-50 side chain rotation due to disruption of the hydrogen bond from Gln-50 to FAD N5 (13, 14).

The correlation between primary photochemical properties and quantum yield of signaling state formation supports the notion that the various BLUF photoreceptors have been evolutionarily adapted for their specific physiological function. Especially, the region around the C2=O carbonyl seems to be a key player for reactivity tuning. So far, the physiologically best-studied BLUF containing protein is AppA, which integrates both light and redox stimuli (5, 6, 76–81). The latter are most likely perceived by a C-terminal cysteine-rich domain and/or a recently discovered novel heme binding domain (82), which is localized between the BLUF domain and the PpsR interaction domain. Both domains are susceptible to redox changes in the environment and are able to induce structural transformations accordingly. The extent to which the redox potential of the environment directly affects the BLUF domain has not been addressed yet. As we observed here, the redox potential of both flavin and tyrosine determines the quantum yield in BLUF photoactivation. If these redox potentials are indirectly coupled to the environment, one may include another redox input into the integrated signal, which originates directly from the BLUF domain. Such a redox relay, however, has not been observed experimentally so far.

In conclusion, we demonstrate that the redox potential of the flavin/tyrosine redox pair in BLUF domains is a key determinant of excited state electron transfer. By modulation of the redox potential, we provide experimental evidence for a previously unobserved excited state charge transfer intermediate prior to electron transfer in the BLUF photocycle. Furthermore, the electron transfer rate correlates with the quantum yield of signaling state formation. Therefore, the redox potential of the tyrosine/flavin redox pair is directly coupled to the biological output. The biological reason for this divergent behavior in excited state decay in various wild type BLUF domains, however, needs to be addressed in future studies.

Acknowledgments—We thank Roman Fudim (Humboldt University, Berlin) for assistance during the measurements and Peter Hegemann (Humboldt University, Berlin) for providing access to his biochemistry facility and general support.

REFERENCES

1. Gomelsky, M., and Klug, G. (2002) BLUF. A novel FAD-binding domain involved in sensory transduction in microorganisms. *Trends Biochem. Sci.* **27,** 497–500
2. Gomelsky, M., and Hoff, W. D. (2011) Light helps bacteria make important lifestyle decisions. *Trends Microbiol.* **19,** 441–448
3. Fiedler, B., Börner, T., and Wilde, A. (2005) Phototaxis in the cyanobacterium Synechocystis sp. PCC 6803. Role of different photoreceptors. *Photochem. Photobiol.* **81,** 1481–1488
4. Ntefidou, M., Iseki, M., Watanabe, M., Lebert, M., and Häder, D.-P. (2003) Photoactivated adenylyl cyclase controls phototaxis in the flagellate *Euglena gracilis*. *Plant Physiol.* **133,** 1517–1521
5. Masuda, S., and Bauer, C. E. (2002) AppA is a blue light photoreceptor that antirepresses photosynthesis gene expression in *Rhodobacter sphaeroides*. *Cell* **110,** 613–623
6. Braatsch, S., Gomelsky, M., Kuphal, S., and Klug, G. (2002) A single flavoprotein, AppA, integrates both redox and light signals in *Rhodobacter sphaeroides*. *Mol. Microbiol.* **45,** 827–836
7. Tschowri, N., Busse, S., and Hengge, R. (2009) The BLUF-EAL protein YcgF acts as a direct anti-repressor in a blue light response of *Escherichia coli*. *Genes Dev.* **23,** 522–534
8. Mussi, M. A., Gaddy, J. A., Cabruja, M., Arivett, B. A., Viale, A. M., Rasia, R., and Actis, L. A. (2010) The opportunistic human pathogen *Acinetobacter baumannii* senses and responds to light. *J. Bacteriol.* **192,** 6336–6345
9. Stierl, M., Stumpf, P., Udwari, D., Gueta, R., Hagedorn, R., Losi, A., Gärtner, W., Petereit, L., Efetova, M., Schwarzel, M., Oertner, T. G., Nagel, G., and Hegemann, P. (2011) Light modulation of cellular cAMP by a small bacterial photoactivated adenylyl cyclase, bPAC, of the soil bacterium Beggiatoa. *J. Biol. Chem.* **286,** 1181–1188
10. Weissenberger, S., Schultheis, C., Liewald, J. F., Erbguth, K., Nagel, G., and Gottschalk, A. (2011) PACα. An optogenetic tool for *in vivo* manipulation of cellular cAMP levels, neurotransmitter release, and behavior in *Caenorhabditis elegans*. *J. Neurochem.* **116,** 616–625
11. Nagahama, T., Suzuki, T., Yoshikawa, S., and Iseki, M. (2007) Functional transplant of photoactivated adenylyl cyclase (PAC) into Aplysia sensory neurons. *Neurosci. Res.* **59,** 81–88
12. Bucher, D., and Buchner, E. (2009) Stimulating PACα increases miniature excitatory junction potential frequency at the *Drosophila* neuromuscular junction. *J. Neurogenet* **23,** 220–224
13. Gauden, M., van Stokkum, I. H., Key, J. M., Lührs, D. C., van Grondelle, R., Hegemann, P., and Kennis, J. T. (2006) Hydrogen bond switching through a radical pair mechanism in a flavin-binding photoreceptor. *Proc. Natl. Acad. Sci. U.S.A.* **103,** 10895–10900
14. Bonetti, C., Mathes, T., van Stokkum, I. H., Mullen, K. M., Groot, M. L., van Grondelle, R., Hegemann, P., and Kennis, J. T. (2008) Hydrogen bond switching among flavin and amino acid side chains in the BLUF photoreceptor observed by ultrafast infrared spectroscopy. *Biophys. J.* **95,** 4790–4802
15. Mathes, T., Zhu, J., van Stokkum, I. H., Groot, M. L., Hegemann, P., and Kennis, J. T. (2012) Hydrogen bond switching among flavin and amino acids determines the nature of proton-coupled electron transfer in BLUF photoreceptors. *J. Phys. Chem. Lett.* **3,** 203–208
16. Kennis, J. T., and Groot, M. L. (2007) Ultrafast spectroscopy of biological photoreceptors. *Curr. Opin. Struct. Biol.* **17,** 623–630
17. Masuda, S., Hasegawa, K., Ishii, A., and Ono, T. A. (2004) Light-induced structural changes in a putative blue light receptor with a novel FAD binding fold sensor of blue light using FAD (BLUF). Slr1694 of *Synechocystis* sp. PCC6803. *Biochemistry* **43,** 5304–5313
18. Hasegawa, K., Masuda, S., and Ono, T. A. (2004) Structural intermediate in the photocycle of a BLUF (sensor of blue light using FAD) protein Slr1694 in a Cyanobacterium *Synechocystis* sp. PCC6803. *Biochemistry* **43,** 14979–14986
19. Grinstead, J. S., Avila-Perez, M., Hellingwerf, K. J., Boelens, R., and Kaptein, R. (2006) Light-induced flipping of a conserved glutamine side chain and its orientation in the AppA BLUF domain. *J. Am. Chem. Soc.* **128,** 15066–15067
20. Unno, M., Sano, R., Masuda, S., Ono, T. A., and Yamauchi, S. (2005) Light-induced structural changes in the active site of the BLUF domain in AppA by Raman spectroscopy. *J. Phys. Chem. B* **109,** 12620–12626
21. Iwata, T., Watanabe, A., Iseki, M., Watanabe, M., and Kandori, H. (2011) Strong donation of the hydrogen bond of tyrosine during photoactivation of the BLUF domain. *J. Phys. Chem. Lett.* **2,** 1015–1019
22. Barends, T. R., Hartmann, E., Griese, J. J., Beitlich, T., Kirienko, N. V., Ryjenkov, D. A., Reinstein, J., Shoeman, R. L., Gomelsky, M., and Schlichting, I. (2009) Structure and mechanism of a bacterial light-regulated cyclic nucleotide phosphodiesterase. *Nature* **459,** 1015–1018
23. Yuan, H., Anderson, S., Masuda, S., Dragnea, V., Moffat, K., and Bauer, C. (2006) Crystal structures of the Synechocystis photoreceptor Slr1694 reveal distinct structural states related to signaling. *Biochemistry* **45,** 12687–12694
24. Jung, A., Reinstein, J., Domratcheva, T., Shoeman, R., and Schlichting, I. (2006) Crystal structures of the AppA BLUF domain photoreceptor provide insights into blue light-mediated signal transduction. *J. Mol. Biol.* **362,** 717–732
25. Kita, A., Okajima, K., Morimoto, Y., Ikeuchi, M., and Miki, K. (2005) Structure of a cyanobacterial BLUF protein, Tll0078, containing a novel FAD-binding blue light sensor domain. *J. Mol. Biol.* **349,** 1–9
26. Jung, A., Domratcheva, T., Tarutina, M., Wu, Q., Ko, W. H., Shoeman, R. L., Gomelsky, M., Gardner, K. H., and Schlichting, I. (2005) Structure of a bacterial BLUF photoreceptor. Insights into blue light-mediated signal transduction. *Proc. Natl. Acad. Sci. U. S. A.* **102,** 12350–12355
27. Anderson, S., Dragnea, V., Masuda, S., Ybe, J., Moffat, K., and Bauer, C. (2005) Structure of a novel photoreceptor, the BLUF domain of AppA from *Rhodobacter sphaeroides*. *Biochemistry* **44,** 7998–8005
28. Sadeghian, K., Bocola, M., and Schütz, M. (2008) A conclusive mechanism of the photoinduced reaction cascade in blue light using flavin photoreceptors. *J. Am. Chem. Soc.* **130,** 12501–12513
29. Domratcheva, T., Grigorenko, B. L., Schlichting, I., and Nemukhin, A. V. (2008) Molecular models predict light-induced glutamine tautomerization in BLUF photoreceptors. *Biophys. J.* **94,** 3872–3879
30. Stelling, A. L., Ronayne, K. L., Nappa, J., Tonge, P. J., and Meech, S. R. (2007) Ultrafast structural dynamics in BLUF domains. Transient infrared spectroscopy of AppA and its mutants. *J. Am. Chem. Soc.* **129,** 15556–15564
31. Udvarhelyi, A., and Domratcheva, T. (2011) Photoreaction in BLUF receptors. Proton-coupled electron transfer in the flavin-Gln-Tyr system. *Photochem. Photobiol.* **87,** 554–563
32. Möglich, A., Yang, X., Ayers, R. A., and Moffat, K. (2010) Structure and function of plant photoreceptors. *Annu. Rev. Plant Biol.* **61,** 21–47
33. Barry, B. A. (2011) Proton-coupled electron transfer and redox active tyrosines in photosystem II. *J. Photochem. Photobiol. B* **104,** 60–71
34. Huynh, M. H., and Meyer, T. J. (2007) Proton-coupled electron transfer. *Chem. Rev.* **107,** 5004–5064
35. Moore, G. F., Hambourger, M., Kodis, G., Michl, W., Gust, D., Moore, T. A., and Moore, A. L. (2010) Effects of protonation state on a tyrosine-histidine bioinspired redox mediator. *J. Phys. Chem. B* **114,** 14450–14457
36. Mathes, T., van Stokkum, I. H., Bonetti, C., Hegemann, P., and Kennis, J. T. (2011) The hydrogen bond switch reaction of the Blrb Bluf domain of *Rhodobacter sphaeroides*. *J. Phys. Chem. B* **115,** 7963–7971
37. Gauden, M., Yeremenko, S., Laan, W., van Stokkum, I. H., Ihalainen, J. A., van Grondelle, R., Hellingwerf, K. J., and Kennis, J. T. (2005) Photocycle of the flavin-binding photoreceptor AppA, a bacterial transcriptional antirepressor of photosynthesis genes. *Biochemistry* **44,** 3653–3662
38. Zirak, P., Penzkofer, A., Schiereis, T., Hegemann, P., Jung, A., and Schlichting, I. (2005) Absorption and fluorescence spectroscopic characterization of BLUF domain of AppA from *Rhodobacter sphaeroides*. *Chem. Phys.* **315,** 142–154
39. Zirak, P., Penzkofer, A., Hegemann, P., and Mathes, T. (2007) Photodynamics of BLUF domain mutant H44R of AppA from *Rhodobacter sphaeroides*. Chemical Physics. *Chem. Phys.* **335,** 15–27
40. Nunthaboot, N., Tanaka, F., and Kokpol, S. (2009) Analysis of photoinduced electron transfer in AppA. *J. Photochem. Photobiol. A* **207,** 274–281
41. Dragnea, V., Waegele, M., Balascuta, S., Bauer, C., and Dragnea, B. (2005) Time-resolved spectroscopic studies of the AppA blue light receptor

BLUF domain from *Rhodobacter sphaeroides*. *Biochemistry* **44,** 15978–15985
42. Shibata, Y., Murai, Y., Satoh, Y., Fukushima, Y., Okajima, K., Ikeuchi, M., and Itoh, S. (2009) Acceleration of electron transfer-induced fluorescence quenching upon conversion to the signaling state in the blue-light receptor, TePixD, from *Thermosynechococcus elongatus*. *J. Phys. Chem. B* **113,** 8192–8198
43. Gauden, M., Grinstead, J. S., Laan, W., van Stokkum, I. H., Avila-Perez, M., Toh, K. C., Boelens, R., Kaptein, R., van Grondelle, R., Hellingwerf, K. J., and Kennis, J. T. (2007) On the role of aromatic side chains in the photoactivation of BLUF domains. *Biochemistry* **46,** 7405–7415
44. Bonetti, C., Stierl, M., Mathes, T., van Stokkum, I. H., Mullen, K. M., Cohen-Stuart, T. A., van Grondelle, R., Hegemann, P., and Kennis, J. T. (2009) The role of key amino acids in the photoactivation pathway of the *Synechocystis* Slr1694 BLUF domain. *Biochemistry* **48,** 11458–11469
45. Ishikita, H. (2007) Influence of the protein environment on the redox potentials of flavodoxins from *Clostridium beijerinckii*. *J. Biol. Chem.* **282,** 25240–25246
46. Ishikita, H. (2008) Light-induced hydrogen bonding pattern and driving force of electron transfer in AppA BLUF domain photoreceptor. *J. Biol. Chem.* **283,** 30618–30623
47. Mathes, T., Vogl, C., Stolz, J., and Hegemann, P. (2009) *In vivo* generation of flavoproteins with modified cofactors. *J. Mol. Biol.* **385,** 1511–1518
48. Datta, S., Costantino, N., and Court, D. L. (2006) A set of recombineering plasmids for gram-negative bacteria. *Gene* **379,** 109–115
49. Datsenko, K. A., and Wanner, B. L. (2000) One-step inactivation of chromosomal genes in *Escherichia coli* K-12 using PCR products. *Proc. Natl. Acad. Sci. U.S.A.* **97,** 6640–6645
50. Mathes, T. (2007) *Photochemie und Signaltransduktion von Blaulichtrezeptorproteinen aus photosynthetisierenden Mikroorganismen.* pp. 62–66, Humboldt University Berlin, Berlin
51. Bordoli, L., Kiefer, F., Arnold, K., Benkert, P., Battey, J., and Schwede, T. (2008) *Nat. Protocols* **4,** 1–13
52. Berera, R., van Grondelle, R., and Kennis, J. T. (2009) Ultrafast transient absorption spectroscopy. Principles and application to photosynthetic systems. *Photosynth. Res.* **101,** 105–118
53. Larsen, D. S., van Stokkum, I. H., Vengris, M., van Der Horst, M. A., de Weerd, F. L., Hellingwerf, K. J., and van Grondelle, R. (2004) Incoherent manipulation of the photoactive yellow protein photocycle with dispersed pump-dump-probe spectroscopy. *Biophys. J.* **87,** 1858–1872
54. Mullen, K. M., and van Stokkum, I. H. (2007) TIMP: An R Package for Modeling Multi-way Spectroscopic Measurements. *J. Stat. Softw.* **18,** 1–46
55. Snellenburg, J. J., Laptenok, S. P., Seger, R., Mullen, K. M., and van Stokkum, I. H. (2012) Glotaran. A Java-based graphical user interface for the R package TIMP. *J. Stat. Softw.* **49,** 1–22
56. Laan, W., Bednarz, T., Heberle, J., and Hellingwerf, K. J. (2004) Chromophore composition of a heterologously expressed BLUF domain. *Photochem. Photobiol. Sci.* **3,** 1011
57. Miura, R. (2001) Versatility and specificity in flavoenzymes. Control mechanisms of flavin reactivity. *Chem. Rec.* **1,** 183–194
58. van den Berg, P. A., van Hoek, A., and Visser, A. J. (2004) Evidence for a novel mechanism of time-resolved flavin fluorescence depolarization in glutathione reductase. *Biophys. J.* **87,** 2577–2586
59. Seyedsayamdost, M. R., Reece, S. Y., Nocera, D. G., and Stubbe, J. (2006) Mono-, di-, tri-, and tetra-substituted fluorotyrosines. New probes for enzymes that use tyrosyl radicals in catalysis. *J. Am. Chem. Soc.* **128,** 1569–1579
60. Ghisla, S., and Massey, V. (1989) Mechanisms of flavoprotein-catalyzed reactions. *Eur. J. Biochem.* **181,** 1–17
61. Fraaije, M. W., and Mattevi, A. (2000) Flavoenzymes. Diverse catalysts with recurrent features. *Trends Biochem. Sci.* **25,** 126–132
62. Arents, J. C., Perez, M. A., Hendriks, J., and Hellingwerf, K. J. (2011) On the midpoint potential of the FAD chromophore in a BLUF domain-containing photoreceptor protein. *FEBS Lett.* **585,** 167–172
63. Grinstead, J. S., Hsu, S. T., Laan, W., Bonvin, A. M., Hellingwerf, K. J., Boelens, R., and Kaptein, R. (2006) The solution structure of the AppA BLUF domain. Insight into the mechanism of light-induced signaling. *Chembiochem* **7,** 187–193
64. Marcus, R. A., and Sutin, N. (1985) Electron transfer in chemistry and biology. *Biochim. Biophys. Acta* **811,** 265–322
65. Grampp, G. (1993) The Marcus inverted region from theory to experiment. *Angew. Chem. Int. Ed. Engl.* **32,** 691–693
66. Thanasekaran, P., Rajendran, T., Rajagopal, S., Srinivasan, C., Ramaraj, R., Ramamurthy, P., and Venkatachalapathy, B. (1997) Marcus inverted region in the photoinduced electron transfer reactions of ruthenium (II)-polypyridine complexes with phenolate ions. *J. Phys. Chem. A* **101,** 8195–8199
67. Porcal, G., Bertolotti, S. G., Previtali, C. M., and Encinas, M. V. (2003) Electron transfer quenching of singlet and triplet excited states of flavins and lumichrome by aromatic and aliphatic electron donors. *Phys. Chem. Chem. Phys.* **5,** 4123–4128
68. Moser, C. C., Page, C. C., Farid, R., and Dutton, P. L. (1995) Biological electron transfer. *J. Bioenerg. Biomembr.* **27,** 263–274
69. Liu, Z., Guo, X., Tan, C., Li, J., Kao, Y. T., Wang, L., Sancar, A., and Zhong, D. (2012) Electron tunneling pathways and role of adenine in repair of cyclobutane pyrimidine dimer by DNA photolyase. *J. Am. Chem. Soc.* **134,** 8104–8114
70. Pal, P. P., Bae, J. H., Azim, M. K., Hess, P., Friedrich, R., Huber, R., Moroder, L., and Budisa, N. (2005) Structural and spectral response of *Aequorea victoria* green fluorescent proteins to chromophore fluorination. *Biochemistry* **44,** 3663–3672
71. Miroux, B., and Walker, J. E. (1996) Overproduction of proteins in *Escherichia coli*. Mutant hosts that allow synthesis of some membrane proteins and globular proteins at high levels. *J. Mol. Biol.* **260,** 289–298
72. Dunitz, J. D. (2004) Organic fluorine. Odd man out. *ChemBioChem* **5,** 614–621
73. Toh, K. C., van Stokkum, I. H., Hendriks, J., Alexandre, M. T., Arents, J. C., Perez, M. A., van Grondelle, R., Hellingwerf, K. J., and Kennis, J. T. (2008) On the signaling mechanism and the absence of photoreversibility in the AppA BLUF domain. *Biophys. J.* **95,** 312–321
74. Weber, S., Schroeder, C., Kacprzak, S., Mathes, T., Kowalczyk, R. M., Essen, L. O., Hegemann, P., Schleicher, E., and Bittl, R. (2011) Light-generated paramagnetic intermediates in BLUF domains. *Photochem. Photobiol.* **87,** 574–583
75. Zirak, P., Penzkofer, A., Schiereis, T., Hegemann, P., Jung, A., and Schlichting, I. (2006) Photodynamics of the small BLUF protein BlrB from *Rhodobacter sphaeroides*. *J. Photochem. Photobiol. B* **83,** 180–194
76. Masuda, S., Tomida, Y., Ohta, H., and Takamiya, K. I. (2007) The critical role of a hydrogen bond between Gln-63 and Trp-104 in the blue light-sensing BLUF domain that controls AppA activity. *J. Mol. Biol.* **368,** 1223–1230
77. van der Horst, M. A., Laan, W., Yeremenko, S., Wende, A., Palm, P., Oesterhelt, D., and Hellingwerf, K. J. (2005) From primary photochemistry to biological function in the blue light photoreceptors PYP and AppA. *Photochem. Photobiol. Sci.* **4,** 688–693
78. Jäger, A., Braatsch, S., Haberzettl, K., Metz, S., Osterloh, L., Han, Y., and Klug, G. (2007) The AppA and PpsR proteins from *Rhodobacter sphaeroides* can establish a redox-dependent signal chain but fail to transmit blue light signals in other bacteria. *J. Bacteriol.* **189,** 2274–2282
79. Braatsch, S., Moskvin, O. V., Klug, G., and Gomelsky, M. (2004) Responses of the *Rhodobacter sphaeroides* transcriptome to blue light under semiaerobic conditions. *J. Bacteriol.* **186,** 7726–7735
80. Metz, S., Jäger, A., and Klug, G. (2009) *In vivo* sensitivity of blue light-dependent signaling mediated by AppA/PpsR or PrrB/PrrA in *Rhodobacter sphaeroides*. *J. Bacteriol.* **191,** 4473–4477
81. Pandey, R., Flockerzi, D., Hauser, M. J., and Straube, R. (2011) Modeling the light- and redox-dependent interaction of PpsR/AppA in *Rhodobacter sphaeroides*. *Biophys. J.* **100,** 2347–2355
82. Han, Y., Meyer, M. H., Keusgen, M., and Klug, G. (2007) A heme cofactor is required for redox and light signaling by the AppA protein of *Rhodobacter sphaeroides*. *Mol. Microbiol.* **64,** 1090–1104

Redox modulation of flavin and tyrosine determines photoinduced proton-coupled electron transfer and photoactivation of BLUF photoreceptors

Tilo Mathes[1], *Ivo H.M. van Stokkum*[1], *Manuela Stierl*[2], *John T.M. Kennis*[1].

[1]Biophysics Group, Department of Physics and Astronomy, Faculty of Sciences, Vrije Universiteit, De Boelelaan 1081, 1081 HV, Amsterdam, The Netherlands,

[2]Institut für Biologie, Experimentelle Biophysik, Humboldt Universität zu Berlin, Invalidenstraße 42, D-10115 Berlin, Germany.

t.mathes@vu.nl

SUPPORTING INFORMATION

The following contains supporting information on the target analysis described in the manuscript.

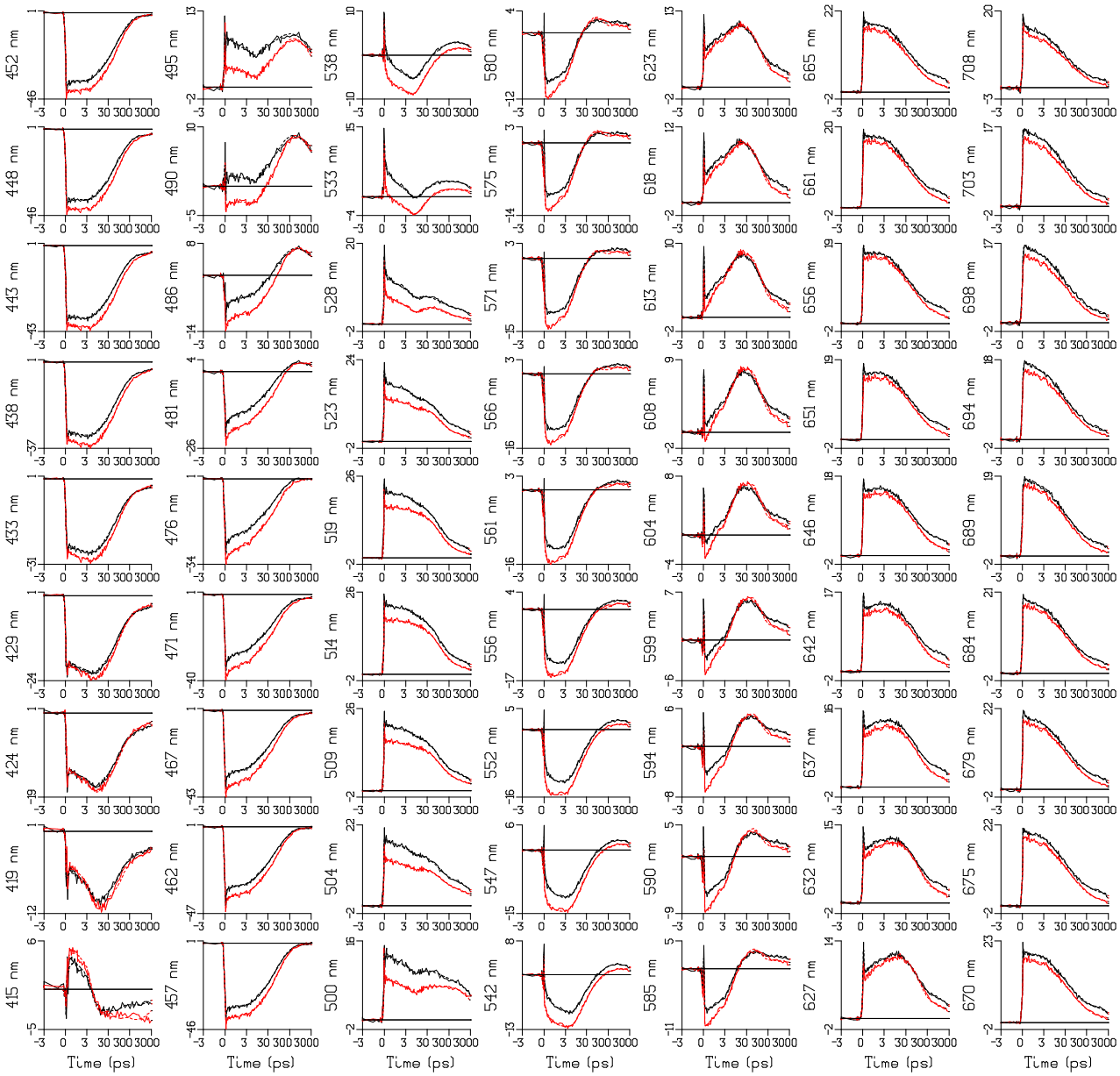

Figure S1, Overview of absorbance change after femtosecond excitation of N31-mutants of Slr1694 in H_2O at selected wavelengths. Key: N31H (black) and N31R (red). The time scale is linear until 3 ps and logarithmic thereafter. The raw data is displayed as a solid line superimposed with the target analysis fit (dashed). Around 495 and 533 nm the traces show the clear formation and decay of stimulated emission of another excited state around 8 ps. At the characteristic wavelengths around 600 nm, the traces show the clear formation of a semiquinone characteristic absorption at around 30 ps, which subsequently decays within 54 (N31H) or 63 (N31R) picoseconds.

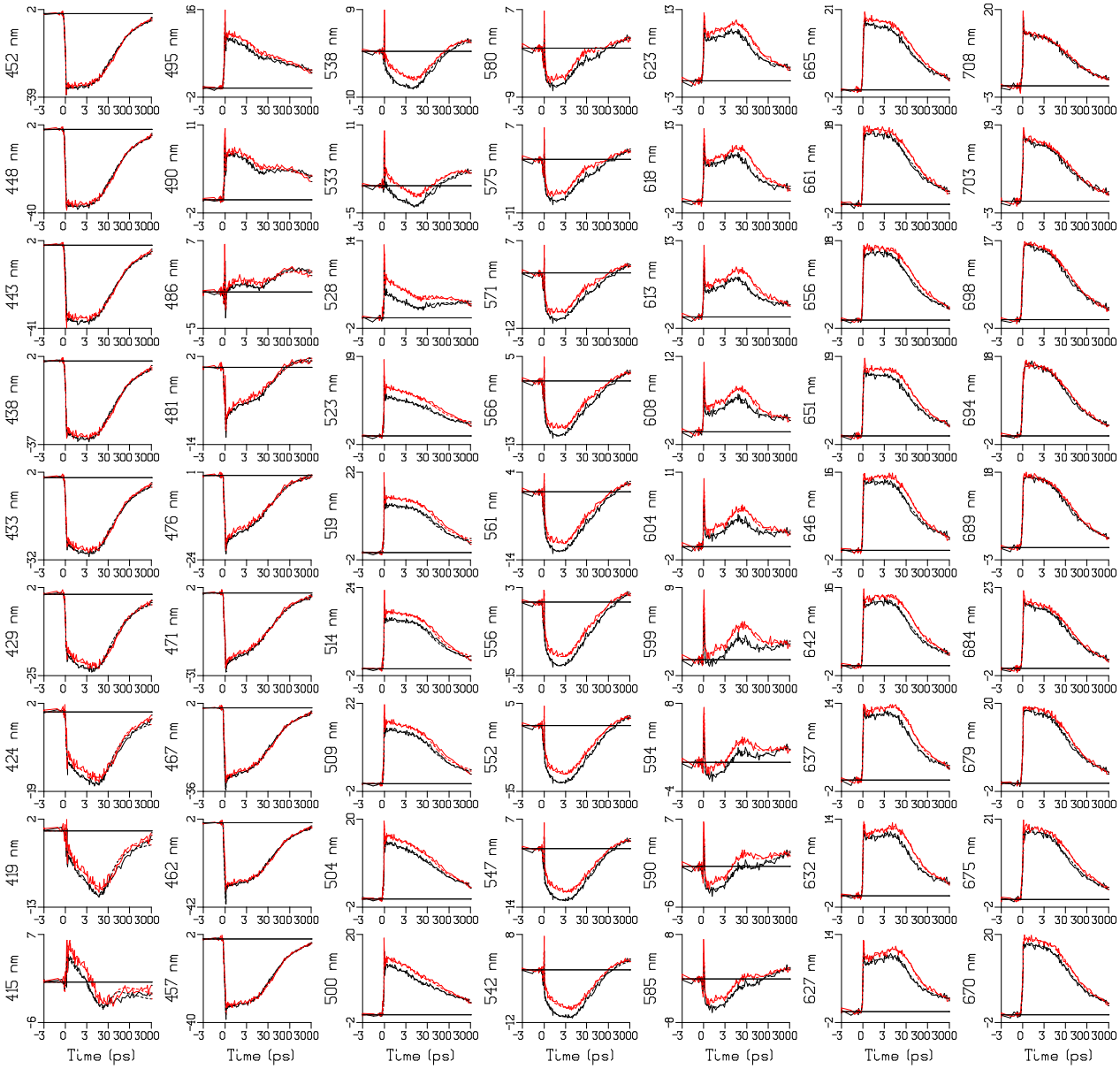

Figure S2, Simultaneous target analysis of SlrY3F in H_2O (black) and D_2O (red). The time scale is linear until 3 ps and logarithmic thereafter. The raw data is displayed as a solid line superimposed with the target analysis fit (dashed). At the characteristic semiquinone wavelengths around 600 nm, a slowed down decay of the D_2O trace is obvious in the raw data. Thus a kinetic isotope effect on the decay of this species is present, with decay times of 16 ps in H_2O and 28 ps in D_2O.

A

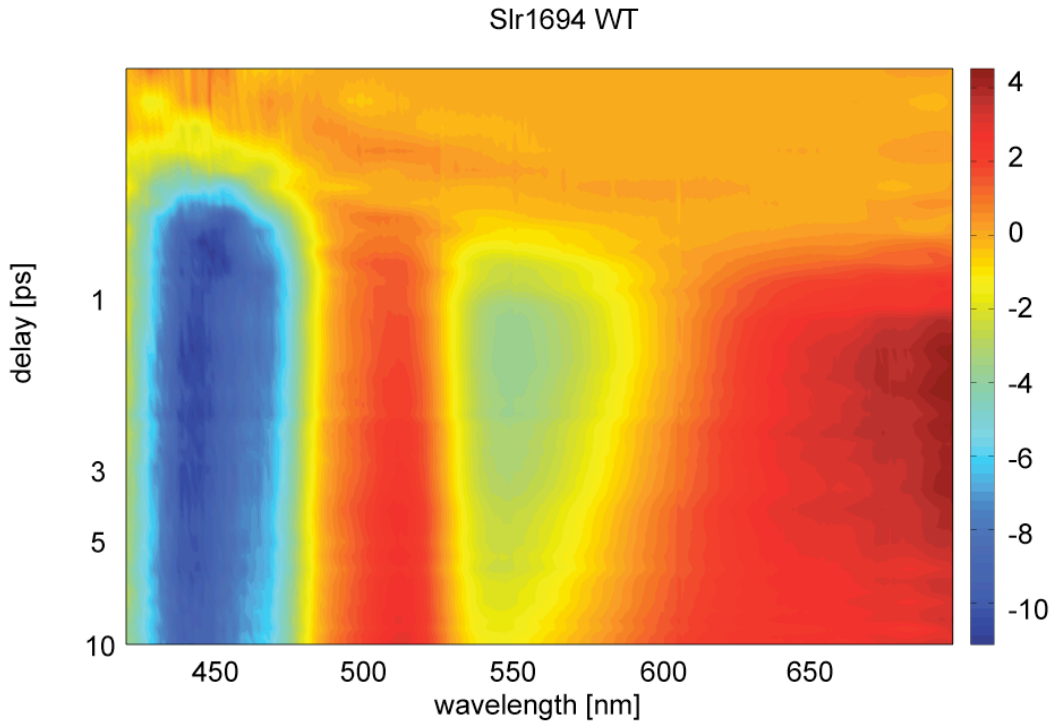

B

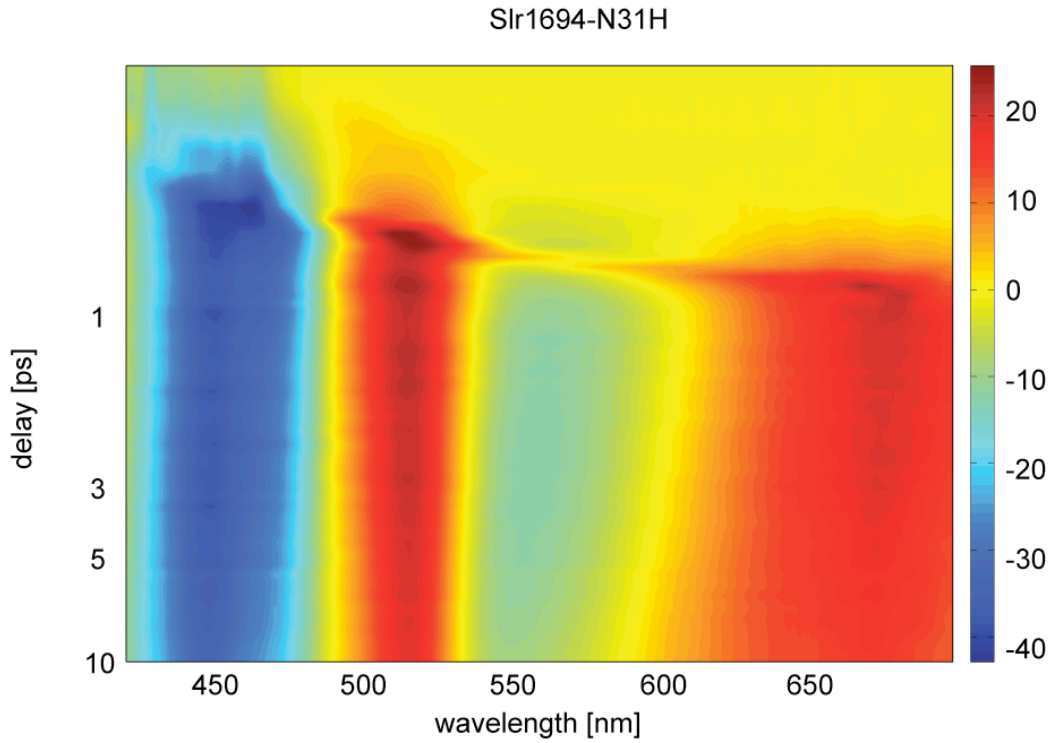

Figure S3, spectral evolution in the first 10 ps on a logarithmic scale after excitation of Slr1694 WT (A) and Slr1694-N31H (B). The decay of SE at around 550 nm is observed in WT significantly within the first 10 ps. In N31H a shift towards shorter wavelengths is observed, thus indicating a newly formed SE feature.

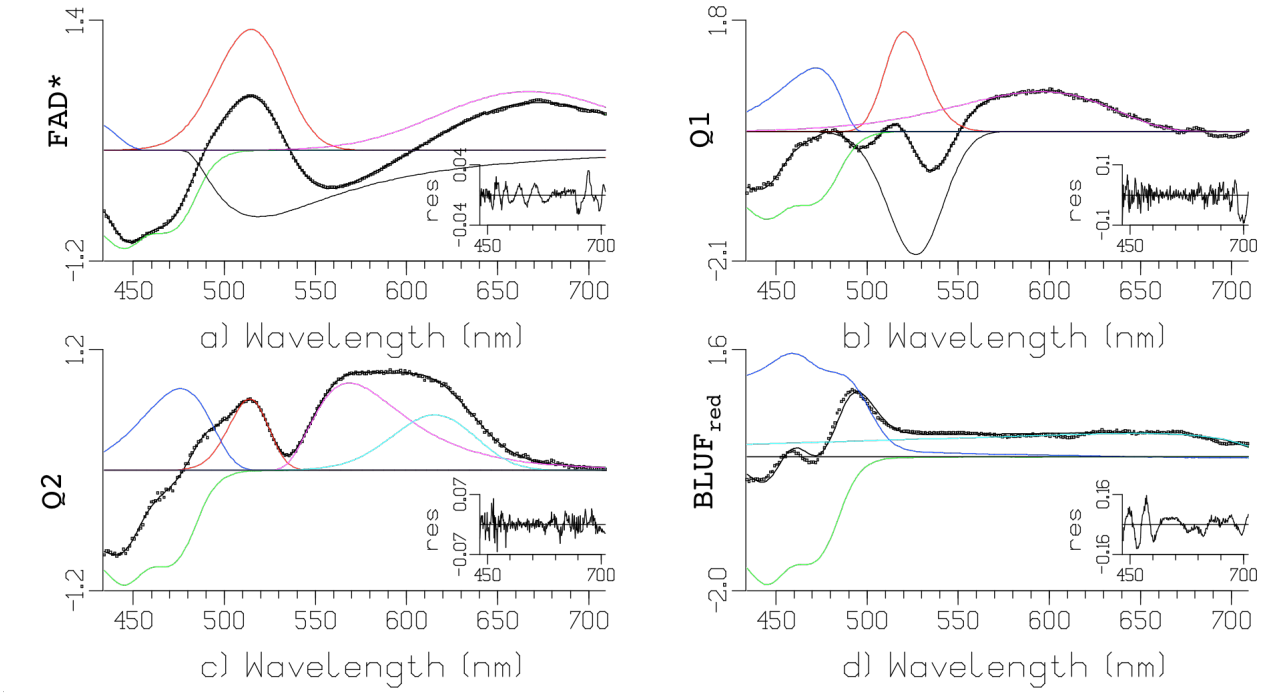

Figure S4, Spectral fit of all the N31H SADS using a bleach (green), and skewed Gaussian bands for stimulated emission (black), and for (excited state) absorption (blue, red, magenta, and cyan).